DMD Fast Forward. Published on December 31, 2018 as DOI: 10.1124/dmd.118.084772
This article has not been copyedited and formatted. The final version may differ from this version.

Commensal gut bacteria convert the immunosuppressant tacrolimus to less potent metabolites

Yukuang Guo[1,5], Camila Manoel Crnkovic[1], Kyoung-Jae Won[2], Xiaotong Yang[4], John Richard Lee[3], Jimmy Orjala[1,5], Hyunwoo Lee[1,5], and Hyunyoung Jeong[2,4,5]

[1,] Department of Medicinal Chemistry and Pharmacognosy, University of Illinois at Chicago

[2,] Department of Pharmacy Practice, University of Illinois at Chicago

[3,] Division of Nephrology and Hypertension, Department of Medicine, Weill Cornell Medicine

[4,] Department of Biopharmaceutical Sciences, University of Illinois at Chicago

[5,] Center for Biomolecular Sciences

Running title: Tacrolimus metabolism by gut bacteria

Correspondence and requests for materials should be addressed to J.O. (for tacrolimus metabolite M1), H.L. (for bacteria), and H.J. (for the rest).

Jimmy Orjala, orjala@uic.edu

Hyunwoo Lee, hlee31@uic.edu

Hyunyoung Jeong, yjeong@uic.edu

College of Pharmacy, University of Illinois at Chicago

900 South Ashland Ave, Chicago, IL 60607

text pages: 26

table: 3

figure: 6

references: 32

words in the Abstract: 199

words in the Introduction: 404

words in the Discussion: 1143

Abbreviations

BEI, biodefense and emerging infections; BrdU, 5-bromo-2'-deoxyuridine: COSY, homonuclear ^{1}H-^{1}H correlation spectroscopy; DEPTQ, distorsionless enhancement by polarization transfer quaternary; HMBC, heteronuclear multiple bond correlation spectroscopy; HPLC, high performance liquid chromatography; HRMS, high resolution mass spectrometry; HSQC, heteronuclear single quantum coherence spectroscopy; IR, infrared spectroscopy; MS/MS, tandem mass spectrometry; NMR, nuclear magnetic resonance spectroscopy; PBMC, oeripheral blood mononuclear cells; P-gp, p-glycoprotein; PHA, phytohemagglutinin; TMB, 3,3′,5,5′-tetramethylbenzidine; TOCSY, total correlated spectroscopy

Abstract

Tacrolimus exhibits low and variable drug exposure after oral dosing, but the contributing factors remain unclear. Based on our recent report showing a positive correlation between fecal abundance of *Faecalibacterium prausnitzii* and oral tacrolimus dose in kidney transplant patients, we tested whether *F. prausnitzii* and other gut abundant bacteria are capable of metabolizing tacrolimus. Incubation of *F. prausnitzii* with tacrolimus led to production of two compounds (the major one named M1), which was not observed upon tacrolimus incubation with hepatic microsomes. Isolation, purification, and structure elucidation using mass spectrometry and nuclear magnetic resonance spectroscopy indicated that M1 is a C-9 keto-reduction product of tacrolimus. Pharmacological activity testing using human peripheral blood mononuclear cells demonstrated that M1 is 15-fold less potent than tacrolimus as an immunosuppressant. Screening of 22 gut bacteria species revealed that most *Clostridiales* bacteria are extensive tacrolimus metabolizers. Tacrolimus conversion to M1 was verified in fresh stool samples from two healthy adults. M1 was also detected in the stool samples from kidney transplant recipients who had been taking tacrolimus orally. Together, this study presents gut bacteria metabolism as a previously unrecognized elimination route of tacrolimus, potentially contributing to the low and variable tacrolimus exposure after oral dosing.

DMD Fast Forward. Published on December 31, 2018 as DOI: 10.1124/dmd.118.084772
This article has not been copyedited and formatted. The final version may differ from this version.

1. Introduction

Tacrolimus is a commonly used immunosuppressant for kidney transplant recipients as well as patients with glomerular diseases like membranous nephropathy and focal segmental glomerulosclerosis. However, due to its narrow therapeutic index, under-exposure or over-exposure to tacrolimus in kidney transplant recipients increases the risks for graft rejection or drug-related toxicity, respectively (Staatz and Tett, 2004). Maintaining therapeutic blood concentrations of tacrolimus has been difficult in part because tacrolimus pharmacokinetics shows large inter-indiviudal and intra-individual variability (Press et al., 2009; Shuker et al., 2015). For example, tacrolimus oral bioavailability in individual patients ranges from 5 to 93% (average ~25%) (Staatz and Tett, 2004). A better understanding of the factors responsible for the variability is crucial for maintaining target therapeutic concentrations of tacrolimus and improving kidney transplant outcomes.

The human gut is home to over trillions of microbes that can influence multiple aspects of host physiology (Schroeder and Backhed, 2016). In particular, intestinal bacteria can mediate diverse chemical reactions such as hydrolysis and reduction of orally administered drugs, ultimately affecting the efficacy and/or toxicity of drugs (Wallace et al., 2010; Haiser et al., 2013; Koppel et al., 2017). For example, digoxin is converted to the pharmacologically inactive metabolite, dihydrodigoxin, by the gut bacterium *Eggerthella lenta* (Haiser et al., 2013). The expression of the enzyme responsible for digoxin metabolism in *E. lenta* is influenced by dietary protein content (Haiser et al., 2013), indicating that in addition to the abundance of drug-metabolizing bacteria, diet composition may also govern the extent of drug metabolism in the gut and alter systemic drug exposure. For most clinically used drugs, the detailed roles of gut bacteria in their metabolism and/or disposition remain unknown.

Faecalibacterium prausnitzii is one of the most abundant human gut bacteria (10^8-10^9 16S rRNA gene copies/g mucosal tissue in ileum and colon), taxonomically belonging to the *Clostridiales* order (Qin et al., 2010; Arumugam et al., 2011). Because of its anti-inflammatory effects, *F. prausnitzii* has been investigated as a potential preventative and/or therapeutic agent for dysbiosis (Miquel et al., 2015; Rossi et al., 2016). We have recently shown that in 19 kidney transplant patients, fecal *F. prausnitzii* abundance

DMD Fast Forward. Published on December 31, 2018 as DOI: 10.1124/dmd.118.084772
This article has not been copyedited and formatted. The final version may differ from this version.

positively correlates with oral tacrolimus doses required to maintain therapeutic blood concentrations, independent of gender and body weight (Lee et al., 2015). It remains unknown, however, whether *F. prausnitzii* is directly involved in tacrolimus elimination in the gut. Herein, we tested a hypothesis that gut bacteria, including *F. prausnitzii*, metabolize tacrolimus into less potent metabolite(s).

2. Materials and Methods

2.1. Reagents. Tacrolimus was purchased from AdipoGen (San Diego, CA). Casitone and yeast extract were purchased from HIMEDIA (Nashik, MH, IN) and BD (Sparks, MD), respectively. Other components for media were purchased from Thermo Fisher Scientific (Waltham, MA) or Sigma-Aldrich (St. Louis, MO).

Peripheral blood mononuclear cells (PBMC; C-12907) were purchased from PromoCell (Heidelberg, Germany). Phytohemagglutinin (PHA; L1668) and 5-bromo-2'-deoxyuridine (BrdU; B9285) were purchased from Sigma-Aldrich. 3,3′,5,5′-Tetramethylbenzidine (TMB; 34022) was purchased from Thermo Fisher Scientific.

2.2. Bacterial strains and growth. *F. prausnitzii* A2-165 was obtained from DSMZ (Deutsche Sammlung von Mikroorganismen und Zellkulturen GmbH). *F. prausnitzii* VPI C13-20-A (ATCC 27766), and *F. prausnitzii* VPI C13-51 (ATCC 27768) were from American Type Culture Collection (ATCC). Other gut bacteria were from Biodefense and Emerging Infections (BEI) Research Resources Repository (Supplemental Table 1). Unless stated otherwise, all the bacterial strains were grown anaerobically (5% H_2, 5% CO_2, 90% N_2) on YCFA agar or broth at 37ºC in an anaerobic chamber (Anaerobe Systems, Morgan Hill, CA), and colonies from the agar plate were inoculated into pre-reduced YCFA broth for preparation of overnight cultures. Optical density at 600 nm (OD_{600}) was measured for estimation of bacterial concentration.

2.3. Tacrolimus metabolism by gut bacteria. To examine tacrolimus metabolism by gut bacteria, cells of a bacterial strain grown as described above were incubated tacrolimus. Typically, tacrolimus (100 μg/ml) was incubated with bacterial cells in the anaerobic chamber at 37ºC for 24-48 h. Reaction was

DMD Fast Forward. Published on December 31, 2018 as DOI: 10.1124/dmd.118.084772
This article has not been copyedited and formatted. The final version may differ from this version.

terminated by adding the same volume of ice-cold acetonitrile. After vortexing for 30 sec, samples were centrifuged at 16,100×*g* for 10 min, and the supernatant was collected for HPLC/UV analysis as described below.

2.4. M1 detection. The reaction mixture was analyzed by using HPLC (Waters 2695) coupled with a UV detector (Waters 2487). Typically, 50 μl of a sample was injected and resolved on a C8 column (Eclipse XDB-C8;4.6 x 250 nm; 5 μm) using water (0.02 M KH_2PO_4, pH 3.5; solvent A) and acetonitrile (solvent B) as mobile phase with the following gradient: 0-12 min (50% B), 12-17 min (50%-70% B), 17-23 min (70% B), 24-30 min (90% B), and 30-40 min (50% B). Eluates were monitored at 210 nm.

For further verification of M1 production by gut bacteria, the supernatant was also analyzed by HPLC tandem mass spectrometry (HPLC/MS/MS), Agilent 1200 HPLC interfaced with Applied Biosystems Qtrap 3200 using an electrospray ion source. The mobile phase consisted of water with 0.1% formic acid and 0.1% ammonium formate (v/v; solvent A) and methanol (solvent B), and the following gradient was used: 0-2 min (40% B), 2-6 min (95% B), and 6-12 min (40% B). Separation was performed on a Xterra MS C18 (2.1 x 50mm, 3.5 μm; Waters) column at a flow rate of 0.3 ml/min, and M1 was detected at *m/z* 828.5/463.5 in the multiple reaction monitoring mode.

2.5. Tacrolimus metabolism by hepatic microsome. Mouse or human hepatic microsomes (purchased from Corning Life Sciences; 3 mg microsomal protein/ml) were incubated with tacrolimus (100 μg/ml) in a reaction mixture (1 mM $NADP^+$, 5 mM $MgCl_2$, 0.2 U/L isocitrate dehydrogenase, and 5 mM isocitric acid) at 37°C for 2 h aerobically. The reaction was terminated by adding the same volume of ice-cold acetonitrile, followed by centrifugation at 16,100×*g* for 10 min, and the supernatant was analyzed by HPLC/UV as described above.

2.6. Purification of the metabolite M1. *F. prausnitzii* cells were harvested from 1 L of an overnight culture grown in YCFA media and resuspended in 500 ml PBS containing 50 mg of tacrolimus. After incubation at 37°C for 4 days, cells were removed by centrifugation and supernatant was collected. The supernatant was extracted twice each with 500 ml of ethyl acetate. The upper organic layer was collected

DMD Fast Forward. Published on December 31, 2018 as DOI: 10.1124/dmd.118.084772
This article has not been copyedited and formatted. The final version may differ from this version.

and evaporated using a rotary evaporator. Dried extracts were then dissolved in 800 µl of methanol and the metabolite M1 was purified using a semi-preparative HPLC coupled with PDA detector (Waters 996) and equipped with a Microsorb 60-C8 Dynamax column (Agilent- R00083311C; 250 x 10 mm). The mobile phase consisted of water (solvent A) and acetonitrile (solvent B), and the following gradient was used: 0-12 min (60% B), 12-17 min (60%-70% B), 17-23 min (70% B), 23-25 min (70%-100% B), 25-35 min (100% B), 35-40 min (100%-60% B), and 40-50% min (60% B). A peak at 19.5 min corresponding to M1 was collected, dried, and subjected to structure determination.

2.7. Infrared (IR) and nuclear magnetic resonance (NMR) spectroscopy. IR spectra were acquired on neat samples using a Thermo-Nicolet 6700 with Smart iTRTM accessory. One dimensional (1D) and 2D NMR spectra were obtained on a Bruker AVII 900 MHz spectrometer equipped with a 5 mm TCI cryoprobe. NMR chemical shifts were referenced to residual solvent peaks ($CDCl_3$ δ_H 7.26 and δ_C 77.16). NMR experiments included ^{1}H NMR, Distorsionless Enhancement by Polarization Transfer Quaternary (DEPTQ), Homonuclear ^{1}H-^{1}H Correlation Spectroscopy (COSY), Heteronuclear Single Quantum Coherence Spectroscopy (HSQC), Heteronuclear Multiple Bond Correlation Spectroscopy (HMBC), and ^{1}H-^{13}C HSQC-Total Correlated Spectroscopy (^{1}H-^{13}C HSQC-TOCSY).

2.8. Mass spectrometry (MS) for M1 identification. Experiments were performed on a Shimadzu ultra performance liquid chromatography mass spectrometry (UPLCMS)-IT-TOF. Samples were run on a C18 column (Phenomenex Kinetex; 50 × 2.1 mm; 1.7 µm) at a flow rate of 0.5 ml/min with water/0.1% formic acid (solvent A) and acetonitrile/0.1% formic acid (solvent B) as mobile phase. Gradient program was set from 20% to 100% B for 7 min, held at 100% for 1 min, and returned to initial conditions for re-equilibration. High resolution mass spectrometry (HRMS) spectra were acquired in both positive and negative modes with a scanning range from 150 to 2000 *m/z*, detector voltage at 1.7 kV, nebulizing gas (N_2) flow at 1.5 L/min, drying gas (N_2) pressure at 130 kPa, CDL temperature at 200°C, and block heater temperature at 200°C. Tandem MS (MS/MS) fragmentation was performed with collision energy (CID) and collision gas set to 50% and frequency set to 45 kHz. Additional MS/MS analyses were performed on an impact II QTOF (Bruker) with a scanning range from 50 to 1500 *m/z*, capillary voltage at 4.5 kV,

DMD Fast Forward. Published on December 31, 2018 as DOI: 10.1124/dmd.118.084772
This article has not been copyedited and formatted. The final version may differ from this version.

nebulizer gas pressure (N_2) at 4 bar, drying gas flow at 12 L/min and temperature at 225°C. The three most intense ions per MS1 were selected for MS2, with active exclusion after three spectra. Each spectrum is an average of 65-100% stepping with CID set at 70 eV.

2.9. Immunosuppressant activity. The immunosuppressant activity of tacrolimus and M1 was determined by measuring proliferation of PBMCs as previously described (Messele et al., 2000) with a slight modification. Briefly, cryopreserved PBMCs were stabilized in RPMI1640 medium containing 10% heat-inactivated fetal bovine serum at 37°C and 5% CO_2 for 24 h. Cells were seeded at 1×10^6 cells/ml in 96-well round bottom plates. After incubation for 24 h, cells were pretreated with tacrolimus, M1, or vehicle for 1 h, followed by treatment with PHA (5 μg/ml) and BrdU (20 μM) for 48 h. Cells were centrifuged at 1000×*g* for 5 min, washed with PBS, and fixed with 4% paraformaldehyde for 15 min. The fixed cells were permeabilized with 0.4% Triton X-100 for 5 min and incubated with 2 N HCl at 37°C for 30 min. After washing with PBS, the cells were incubated with 100 mM borate buffer (pH 8.0) for 10 min and washed again with PBS. After blocking with 2% BSA for 1 h, cells were incubated with horseradish peroxidase (HRP)-conjugated BrdU antibody (BU1/75, ICR1) for 1 h at room temperature. Cells were then washed with PBS and incubated with TMB (a HRP substrate) for 30 min. The reaction was stopped by adding 2 N HCl. The absorbance was measured at 450 nm on a plate reader (BioTek, Winooski, VT).

2.10. Antifungal assay. The antifungal activity of tacrolimus and M1 was examined as previously described (Ianiri et al., 2017). Briefly, *Malassezia sympodialis* M1154/77 (a gift from Dr. Joseph Heitman, Duke University) grown overnight in modified Dixon (mDixon) medium at 37°C was plated on mDixon agar. After 1 h incubation, an aliquot (3 μl) of tacrolimus or M1 at different concentrations was spotted on top of the agar, and incubated at 37°C for 2 days. The agar plates were visually inspected, and the images were taken using a camera.

2.11. Healthy volunteers' stool samples. Fresh stool samples from healthy adults (100 mg wet weight/ml) were incubated with tacrolimus (100 μg/ml) anaerobically for 48 h at 37°C. As controls, the stool samples were boiled for 10 min and then incubated with tacrolimus. The incubation mixtures were

analyzed by HPLC/UV as described above. The study protocol for human stool sample collection was approved by the Institutional Review Board at the University of Illinois at Chicago (protocol number 2018-0810).

2.12. Kidney transplant recipients' stool samples. Stool samples were collected from ten kidney transplant recipients during the first month after transplantation at Weill Cornell Medicine and stored at -80°C until analysis. Tacrolimus dosing in each patient was adjusted to achieve a target therapeutic level of 8 to 10 ng/ml. The study protocol for kidney transplant stool sample collection was approved by the Institutional Review Board at Weill Cornell Medicine (protocol number 1207012730).

The microbiota composition of the stool samples was determined using 16S rRNA gene deep sequencing as previously described (Lee et al., 2018). In brief, DNA from stool samples was isolated using a phenol chloroform bead-beater extraction method. The V4-V5 hypervariable region was amplified by PCR and the fragments were sequenced on an Illumina MiSeq (250 x 250 bp). 16S rRNA gene paired-end reads were analyzed using UPARSE (Edgar, 2013) and taxonomic classification was performed using a custom Python script incorporating BLAST (Altschul et al., 1990) with NCBI RefSeq (Tatusova et al., 2014) as a reference training set.

For the measurement of baseline levels of tacrolimus and M1 in stool samples, an aliquot of stool samples was suspended in PBS (final concentration 20 mg/ml). Also, to measure the capacity of stool samples to produce M1, an aliquot of stool samples was suspended in PBS (10 mg/ml) and incubated with tacrolimus anaerobically for 24 h at 37°C. These samples were mixed with 5 volumes of acetonitrile containing ascomycin as an internal standard. An aliquot (10 μl) was injected into Agilent 1290 UPLC coupled with Applied Biosystems Qtrap 6500. The mobile phase consisted of water with 0.1% formic acid and 10 mM ammonium formate (solvent A) and methanol (solvent B), and the following gradient was used: 0-2 min (20% B), 2-5 min (90% B), and 5-8 min (20% B). Separation was performed on an Xterra MS C18 column (2.1x50 mm, 3.5 μm: Waters) at a flow rate of 0.3 ml/min, with the column temperature set at 50°C. M1, tacrolimus, and ascomycin were detected at *m/z* 828.5/463.4, 821.6/768.6,

DMD Fast Forward. Published on December 31, 2018 as DOI: 10.1124/dmd.118.084772
This article has not been copyedited and formatted. The final version may differ from this version.

and 809.5/756.5, respectively, in the multiple reaction monitoring mode. Standard curves (2–100 ng/ml for both tacrolimus and M1) were prepared by spiking tacrolimus or M1 into the stool samples of healthy volunteers.

2.13. Estimation of the extent of tacrolimus metabolism by intestinal bacteria. *F. prausnitzii* was grown overnight in YCFA medium. The overnight culture typically reaches an optical density at 600 nm (OD_{600}) of ~2, which corresponds to ~1.6×10^8 *F. prausnitzii* cells/ml. Cells were harvested by centrifugation at 2,000 × g for 5 min re-suspended in PBS, and serially diluted in PBS (OD_{600} 0.02, 0.2, 0.4, 0.8, 1.6, and 2). To determine the relationship between the number of bacterial cells and the extent of M1 formation, the cell suspensions at different densities were incubated with tacrolimus (10 μg/ml) at 37°C for 2 h under anaerobic conditions. The reaction was stopped by adding 4 volumes of ice-cold acetonitrile containing ascomycin as an internal standard. After vortexing (1 min) and centrifugation at 16,100×*g* (10 min), the supernatant (2 μl) of each sample was injected into HPLC/MS/MS (Agilent 1200 HPLC interfaced with Applied Biosystems Qtrap 3200) and M1 concentrations were determined as described above. To examine the relationship between incubation time and M1 formation, *F. prausnitzii* cells (OD_{600} 0.8, equivalent to 6.3×10^7 cells/ml) in PBS were incubated with tacrolimus (10 μg/ml) for different time (0.5, 1, 2, 4, 8, and 24 h), and M1 formation was determined as described above. To examine the relationship between tacrolimus concentrations and M1 formation, tacrolimus at different concentrations (2, 10, 20, 40, and 50 μg/ml) was incubated with *F. prausnitzii* cells (OD_{600} 0.8) for 1 h, and M1 formation was determined as described above. Assuming that the capabilities of bacteria in human small intestine to produce M1 are similar to that of *F. prausnitzii* cells in PBS, the total amount of M1 formed in the small intestine was estimated as previously reported (McCabe et al., 2015) with modifications:

$$\text{M1 formation rate in vitro (μg/cells/h)} = \frac{\text{Amount of M1 formed (μg)}}{\text{bacterial cell number} \times \text{incubation time (h)}} \quad \text{(eq. 1)}$$

Amount of M1 formed in human small intestine

= M1 formation rate in vitro × total number of bacterial cells × small intestinal transit time (h) (eq. 2)

DMD Fast Forward. Published on December 31, 2018 as DOI: 10.1124/dmd.118.084772
This article has not been copyedited and formatted. The final version may differ from this version.

The value of 4×10^{10} cells was used as the total number of bacteria in small intestine (Sender et al., 2016), and 3.3 h was used as small intestine transit time (Yu et al., 1996).

2.14. Statistical analysis. Statistical analyses for comparison between two groups were performed using Wilcoxon rank sum testing. Correlational analysis between two continuous variables was performed using Spearman correlation. A p-value ≤ 0.05 was considered statistically significant. All statistical analyses were performed using R version 3.3.1 and R studio version 0.99.902.

3. Results

3.1. *F. prausnitzii* potentially metabolizes tacrolimus. To determine whether *F. prausnitzii* is capable of metabolizing tacrolimus, cells of *F. prausnitzii* A2-165 strain grown overnight (in YCFA media) was incubated with tacrolimus (100 μg/ml; 124 μM) anaerobically at 37°C. After 48 h incubation, the mixture was resolved using HPLC and analyzed by a UV detector. The HPLC chromatogram of intact tacrolimus showed multiple peaks, demonstrating tautomer formation as previously reported (Namiki et al., 1993) (Fig. 1A). For estimation of a concentration of intact tacrolimus, the area of the largest peak at retention time 19.7 min was used. After 24 h incubation with *F. prausnitzii*, the concentration of tacrolimus was decreased by ~50% (Fig. 1B), which was accompanied by appearance of two new peaks (designated M1 and M2, Fig. 1A). The M1 and M2 peaks were not observed when tacrolimus was incubated with boiled *F. prausnitzii* cells (Fig. 1A), indicating that the production of M1 and M2 requires live bacterial cells. Similarly to strain A2-165, two additional strains of *F. prausnitzii* (ATCC 27766 and ATCC 27768) were found to produce M1 and M2 (Supplemental Fig. 1), suggesting that this function is likely conserved in different strains of *F. prausnitzii*.

3.2. M1 is a C9 keto-reduction metabolite of tacrolimus. To gain insight into the chemical identity of M1 and M2, high resolution mass spectrometry (HRMS) and HPLC/MS/MS experiments were performed. The *m/z* values of M1 and M2 were $[M+Na]^+$ 828.4846 and 846.4974, respectively, which are consistent with the formulas $C_{44}H_{71}NO_{12}Na$ (with calculated mass of 828.4874 Da) for M1 (Supplemental

DMD Fast Forward. Published on December 31, 2018 as DOI: 10.1124/dmd.118.084772
This article has not been copyedited and formatted. The final version may differ from this version.

Fig. 2) and $C_{44}H_{73}NO_{13}Na$ (with calculated mass of 846.4980 Da) for M2. The calculated formulas suggested M1 to be a reduction product of tacrolimus (i.e., addition of 2H to the parent tacrolimus) and M2 to be a tautomer of M1. The fragmentation pattern of M1 as compared to that of tacrolimus indicated that M1 is likely a keto-reduction product of tacrolimus (Supplemental Fig. 2 and 3).

For structural elucidation, we focused on the major product M1. M1 was mass produced by incubating large amounts of tacrolimus with *F. prausnitzii,* followed by purification using preparative HPLC. The chemical structure of M1 was then determined using various spectroscopic methods. Of note, when the purified M1 was re-injected into HPLC/UV, it resolved into multiple peaks (including one corresponding to M2), indicative of isomerization and/or tautomerization of M1 into M2 (Supplemental Fig. 4). IR spectroscopy further supported that M1 is a product of a carbonyl reduction from tacrolimus (Supplemental Fig. 5). Major differences were observed in the C=O and O-H stretch regions of the IR spectra. NMR spectra showed three major isomers of M1 in $CDCl_3$, for which all resonances were assigned (Supplemental Table 3-5). Detailed analysis of 1D and 2D NMR spectra revealed the site of carbonyl reduction at C-9 and the identity of M1 to be 9-hydroxy-tacrolimus (Supplemental Fig. 6-12). In particular, analysis of the DEPTQ spectrum of M1 revealed the absence of the resonances associated with the carbonyl carbon C-9 found in tacrolimus (δ_C 196.3 for the major isomer, 192.7 for the minor isomer) (Supplemental Fig. 13). Instead, three resonances consistent with the reduction of the carbonyl at C-9 to an alcohol were observed at δ_C 73.0 (isomer I), 68.4 (isomer II), and 69.7 ppm (isomer III). These resonances were associated with protons at δ_H 4.02, 4.51, and 4.37 ppm, respectively, in the HSQC spectrum. In turn, the latter resonances showed COSY correlations to exchangeable protons (δ_H 4.23, 3.21, and 3.58, respectively). HMBC correlations from H-9 to C-8 and C-10 were observed (Supplemental Tables 3-5), supporting the assignment of M1 as 9-hydroxy-tacrolimus. These results establish the structure of M1 as the C-9 keto-reduction product of tacrolimus (Fig. 2).

3.3. M1 is a less potent immunosuppressant than tacrolimus. We compared the activities of M1 and tacrolimus by measuring PBMC proliferation after treatment with T-lymphocyte mitogen PHA (Messele et al., 2000). The 50% inhibitory concentration (IC_{50}) of M1 was 1.97 nM whereas IC_{50} of

DMD Fast Forward. Published on December 31, 2018 as DOI: 10.1124/dmd.118.084772
This article has not been copyedited and formatted. The final version may differ from this version.

tacrolimus was 0.13 nM, demonstrating that M1 was ~15-fold less potent than the parent tacrolimus in inhibiting T-lymphocyte proliferation (Fig. 3A). Tacrolimus is known to exhibit antifungal activity via the same mechanism for immunosuppression (Steinbach et al., 2007). To further examine the pharmacological activity of M1, an antifungal assay was performed. An aliquot of M1 or tacrolimus was placed onto a lawn of the yeast *Malassezia sympodialis*, and their antifungal activities were estimated based on the size of halo formed. M1 was about 10 to 20-fold less potent than tacrolimus in inhibiting the yeast growth (Fig. 3B), consistent with the results obtained from the PBMC proliferation assay. Taken together, these results demonstrate that M1 is less potent as an immunosuppressant and antifungal agent than the parent drug tacrolimus is.

3.4. Tacrolimus is metabolized by a wide range of commensal gut bacteria. To determine whether other gut bacteria can produce M1/M2 from tacrolimus, we obtained 22 human gut bacteria from BEI Research Resources Repository (Supplemental Table 1) and tested them for potential tacrolimus metabolism. The tested bacteria include those belonging to major orders that are known to be highly abundant in the human gut (Qin et al., 2010; Arumugam et al., 2011). Bacteria grown overnight in YCFA media anaerobically were incubated with tacrolimus (100 μg/ml) for 48 h, and the mixtures were analyzed by HPLC/UV. Apparently, gut bacteria in the orders of *Clostridiales* and *Erysipelotrichales,* but not those in *Bacteroidales* and *Bifidobacteriales* produced M1 (Table 1 and Fig. 4A). To further verify the results, the mixtures were re-analyzed by HPLC/MS/MS which exhibits higher sensitivity than HPLC/UV. M1 production by bacteria in *Clostridiales* was verified (a representative chromatogram of *Clostridium citroniae* shown in Supplemental Fig. 14). M1 production by bacteria in *Bacteroidales* was detectable by HPLC/MS/MS albeit at ~100-fold lower levels than that by bacteria in *Clostridiales* (Supplemental Fig. 14). M1 peak was not detected upon tacrolimus incubation with *Bifidobacterium longum* (Supplemental Fig. 14). The formation of M1 was not observed when tacrolimus was incubated with either human or mouse hepatic microsomes (Fig. 4B; also verified by HPLC/MS/MS, data not shown), suggesting that M1 is uniquely produced by gut bacteria.

DMD Fast Forward. Published on December 31, 2018 as DOI: 10.1124/dmd.118.084772
This article has not been copyedited and formatted. The final version may differ from this version.

To examine whether tacrolimus metabolism is indeed mediated by human gut microbiota, fresh stool samples from two healthy adults were incubated with tacrolimus, and M1 production was assessed. Both stool samples produced M1, whereas the control stool samples that were boiled prior to tacrolimus incubation did not (Fig. 5). Taken together, these results show that commensal gut bacteria belonging to different genera metabolize tacrolimus into the less potent M1 metabolite.

3.5. M1 is detected in transplant patients stool samples. *F. prausnitzii* is one of the most abundant human gut bacteria species (Qin et al., 2010; Arumugam et al., 2011), and its fecal abundance was shown to have a positive correlation with oral tacrolimus dosage (Lee et al., 2015). To explore a potential role of *F. prausnitzii* in tacrolimus metabolism in kidney transplant recipients, we evaluated 10 stool samples from kidney transplant recipients who were taking oral tacrolimus (demographic information provided in Table 2 and Supplemental Table 2). Based upon the sequencing results of the V4-V5 hypervariable region of the 16S rRNA gene in stool samples, we selected 5 kidney transplant recipients whose stool samples had a relative gut abundance of *F. prausnitzii* greater than 25% (designated as "high *F. prausnitzii"* group) and 5 kidney transplant recipients whose stool samples showed no to little (if any) presence of *F. prausnitzii* ("low *F. prausnitzii*" group). We first determined the baseline levels of tacrolimus and M1 in the stool samples. We were able to measure baseline tacrolimus levels in eight of the ten stool samples, but we did not detect a significant difference in the baseline tacrolimus level between the high *F. prausnitzii* group and the low *F. prausnitzii* group (median 0.63 vs. 0.29 ng/mg, respectively, $p = 0.46$). We were also able to measure baseline M1 levels in five of the ten stool samples, but we did not detect a significant difference in the baseline M1 level between the high *F. prausnitzii* group and the low *F. prausnitzii* group (median 0.12 vs. <0.1 ng/mg, respectively, $p = 0.48$). Next, we tested the stool samples of both high and low *F. prausnitzii* groups for the capability of M1 production by incubating each of them with tacrolimus (10 μg/ml) for 24 h. M1 production was detected in all ten samples, but the amount produced was similar between the high and low *F. prausnitzii* groups (median 4.5 vs. 7.1 ng/mg, respectively, $p = 0.31$). The 16S rDNA sequencing analysis revealed that gut bacteria belonging to the *Clostridiales* order (a main group of bacteria that are expected to produce the majority of M1) were

DMD Fast Forward. Published on December 31, 2018 as DOI: 10.1124/dmd.118.084772
This article has not been copyedited and formatted. The final version may differ from this version.

highly abundant in all ten samples (Table 2). However, the relative abundance of neither *F. prausnitzii* (Rho = -0.36, $p = 0.31$) nor *Clostridiales* (Rho = 0.44, $p = 0.20$) showed a significant correlation with M1 production. Oral tacrolimus doses (to maintain therapeutic blood concentrations) were similar between the high and the low *F. prausnitzii* groups (median 6 vs. 4 mg/day, respectively, $p = 0.34$) (Table 2).

3.6. Extensive tacrolimus metabolism may occur in human small intestine. For gross estimation of the extent of tacrolimus metabolism in human small intestine, M1 production kinetic profiles were obtained using *F. prausnitzii* as a model bacterium. M1 production increased linearly with the incubation time of up to 4 h (Fig. 6A) and the amount of *F. prausnitzii* up to 1.2×10^8 cells/ml (Fig. 6B). M1 production increased with the increasing concentrations of tacrolimus (Fig. 6C) and did not reach a plateau at the highest concentration tested (50 μg/ml; a concentration attained when a typical tacrolimus oral dose 5 mg is dissolved in 100 ml water). Based on the assumption that bacteria in human small intestine exhibit M1 production capabilities similar to that of *F. prausnitzii* in PBS, the extent of M1 production in small intestine (at 50 μg/ml tacrolimus concentration) was estimated to be 1.9 mg.

4. Discussion

In this study, we have demonstrated that a wide range of commensal gut bacteria can metabolize tacrolimus into a novel metabolite M1 (9-hydroxy-tacrolimus). To the best of our knowledge, this represents the first experimental evidence for commensal gut bacteria being involved in the metabolism of tacrolimus.

The extent of M1's contribution to overall immunosuppression by tacrolimus therapy is unclear. M1 is ~15-fold less potent than tacrolimus in inhibiting both the proliferation of activated T-lymphocytes and the growth of the yeast *M. sympodialis*. This result is consistent with the currently available structure-activity relationships of tacrolimus analogs; modifications at the C-9 position affect the interaction of tacrolimus with its effector protein (i.e., FK506 binding protein 12) and lead to decreased immunosuppressant activities (Goulet et al., 1994). While the systemic concentrations of M1 after oral tacrolimus dosing remain to be measured, results from previous tacrolimus disposition studies using a

DMD Fast Forward. Published on December 31, 2018 as DOI: 10.1124/dmd.118.084772
This article has not been copyedited and formatted. The final version may differ from this version.

radiolabeled compound (Moller et al., 1999) indicate that the blood concentrations of metabolites are likely lower than that of tacrolimus. These results suggest that pharmacological activity originated from circulating M1 is likely less than that from tacrolimus. Of note, certain tacrolimus metabolites (e.g., 13-*O*-demethyltacrolimus), independently of their immunosuppressive activities, cross-react with the antibodies used in the immunoassays for measurement of tacrolimus blood concentrations, leading to overestimation of tacrolimus concentrations (Staatz and Tett, 2004; Dubbelboer et al., 2012). Interestingly, the extent of such overestimation could not be fully explained by the cross-reactivity of currently known tacrolimus metabolites (Dubbelboer et al., 2012). Whether the novel metabolite M1 cross-reacts with the antibodies, accounting in part for the overestimation of tacrolimus concentrations, is currently being investigated.

Multiple factors have been reported to contribute to the low and variable bioavailability of orally administered tacrolimus. These include differential expression and/or activity levels of cytochrome P450 enzymes (especially CYP3A4 and CYP3A5 isoforms) and the drug transporter P-glycoprotein (P-gp) in the intestine and liver (Staatz and Tett, 2004). Previous pharmacokinetics studies in healthy volunteers and renal transplant recipients have shown that hepatic extraction of tacrolimus is very low (i.e., 4-8%) (Floren et al., 1997; Tuteja et al., 2001), suggesting that the low oral bioavailability of tacrolimus is mainly due to drug loss in the gut. P-gp-mediated drug efflux and intestinal CYP3A-mediated metabolism were proposed as major contributors to the loss. However, results from drug-drug interaction studies have shown that oral bioavailability of tacrolimus increases to at most ~30% when co-administered with ketoconazole, a potent inhibitor of CYP3As and P-gp (Floren et al., 1997; Tuteja et al., 2001); 70% of oral dose is lost (not reaching systemic circulation) even when intestinal CYP3A and P-gp activities are blocked by ketoconazole. Our results suggest that tacrolimus conversion to M1 in the gut may represent a previously unrecognized pathway of tacrolimus elimination in the gut, potentially contributing to tacrolimus loss in the gut.

We attempted to estimate the overall magnitude of tacrolimus metabolism in the human small intestine using *F. prausnitzii* as a model gut bacterium. *F. prausnitzii* was chosen because it is one of the most abundant bacterium (at the bacterial species level) in the human gut including the small intestine

(Sokol et al., 2008; Qin et al., 2010; Lopez-Siles et al., 2015). Our estimation indicates that about 1.9 mg of M1 may be produced in the small intestine during drug transit through the organ. Considering that the typical oral dose of tacrolimus ranges from 2 to 5 mg, a significant fraction of the orally administered tacrolimus may be lost by gut bacterial metabolism before absorption. On the other hand, it should be noted that our calculation may grossly overestimate or underestimate the true extent of tacrolimus metabolism in the gut because (1) bacterial gene expression (and thereby function) in the gut is likely different from that in the laboratory medium used in our study; (2) the capacity of other gut bacteria to metabolize tacrolimus may be widely different as compared to that of *F. prausnitzii*; and (3) a low solubility drug such as tacrolimus may reach the lower gastrointestinal tract (Sousa et al., 2008) and be presented to a large amount of gut bacteria in the colon. Slow absorption of tacrolimus over a prolonged period has been reported clinically (Venkataramanan et al., 1995). Studies are currently ongoing to measure the extent of tacrolimus metabolism by gut bacteria in mice.

Our results revealed that multiple commensal gut bacteria are capable of metabolizing tacrolimus, suggesting that differences in gut bacterial composition may lead to differential tacrolimus exposure in kidney transplant recipients. Gut bacteria that extensively metabolized tacrolimus into M1 (including *F. prausnitzii*) belong to the *Clostridiales* order. On the other hand, bacteria in *Bacteroidales* were found to be weak producers of M1 (i.e., detectable only by sensitive HPLC/MS/MS), and *B. longum* in *Bifidobacteriales* did not produce detectable amounts of M1. A previous study has shown that fecal abundance of *F. prausnitzii* (belonging to *Clostridiales* order) was positively correlated with oral tacrolimus dose in 19 kidney transplant patients (Lee et al., 2015). However, we observed no differences in M1 production between high and low *F. prausnitzii* groups of stool samples. Also, we did not observe correlation between *Clostridiales* abundance and M1 production in the stool samples. This may be due to the small number of samples used for this exploratory study and/or the quality of samples non-optimal for enzymatic assays. The presence of multiple factors affecting gut bacterial gene expression *in vivo* such as nutritional status of the gut may further explain why we do not observe a correlation between our *in vitro* culture-based results and *in vivo* abundance of gut bacteria. For example, the amino acid arginine was

shown to repress the expression of the gene encoding digoxin-metabolizing enzyme in *E. lenta*, thus reducing digoxin elimination by gut bacteria (Haiser et al., 2013). Obviously, *in vitro* culture-based systems do not fully reflect the bacterial functions activated in the physiological gut ecosystem. In this regard, our follow-up study is focused on the identification of the bacterial gene(s) responsible for tacrolimus metabolism. Such information will enable us to examine the prevalence and abundance of tacrolimus-metabolizing enzymes in gut bacterial community and identify factors such as diet or drugs that alter gut bacterial composition and/or gene expression that are specific for tacrolimus metabolism.

In summary, we present the evidence of tacrolimus metabolism by gut bacteria, providing potential explanations for its low oral bioavailability. Tacrolimus metabolism into M1 may represent a novel elimination pathway that occurs before intestinal absorption of tacrolimus. While the extent of gut metabolism of tacrolimus on variable tacrolimus exposure remains to be determined, our data provide a novel understanding of tacrolimus metabolism and may explain variability in tacrolimus exposures in kidney transplant recipients and patients with glomerular diseases on tacrolimus therapy.

Acknowledgment

We thank Joseph Heitman (Duke University) for kindly providing the yeast strain, and Jennifer C. Chang for proofreading the manuscript.

Author Contributions

Participated in research design: Guo, Crnkovic, Won, Yang, J. Lee, Orjala, H. Lee, and Jeong

Conducted experiments: Guo, Crnkovic, Won, and Yang

Performed data analysis: Guo, Crnkovic, Won, Yang, J. Lee, Orjala, H. Lee, and Jeong

Wrote or contributed to the writing of the manuscript: Guo, Crnkovic, Won, Yang, J. Lee, Orjala, H. Lee, and Jeong

References

Altschul SF, Gish W, Miller W, Myers EW, and Lipman DJ (1990) Basic local alignment search tool. *J Mol Biol* **215:**403-410.

Arumugam M, Raes J, Pelletier E, Le Paslier D, Yamada T, Mende DR, Fernandes GR, Tap J, Bruls T, Batto JM, Bertalan M, Borruel N, Casellas F, Fernandez L, Gautier L, Hansen T, Hattori M, Hayashi T, Kleerebezem M, Kurokawa K, Leclerc M, Levenez F, Manichanh C, Nielsen HB, Nielsen T, Pons N, Poulain J, Qin J, Sicheritz-Ponten T, Tims S, Torrents D, Ugarte E, Zoetendal EG, Wang J, Guarner F, Pedersen O, de Vos WM, Brunak S, Dore J, Meta HITC, Antolin M, Artiguenave F, Blottiere HM, Almeida M, Brechot C, Cara C, Chervaux C, Cultrone A, Delorme C, Denariaz G, Dervyn R, Foerstner KU, Friss C, van de Guchte M, Guedon E, Haimet F, Huber W, van Hylckama-Vlieg J, Jamet A, Juste C, Kaci G, Knol J, Lakhdari O, Layec S, Le Roux K, Maguin E, Merieux A, Melo Minardi R, M'Rini C, Muller J, Oozeer R, Parkhill J, Renault P, Rescigno M, Sanchez N, Sunagawa S, Torrejon A, Turner K, Vandemeulebrouck G, Varela E, Winogradsky Y, Zeller G, Weissenbach J, Ehrlich SD, and Bork P (2011) Enterotypes of the human gut microbiome. *Nature* **473:**174-180.

Dubbelboer IR, Pohanka A, Said R, Rosenborg S, and Beck O (2012) Quantification of tacrolimus and three demethylated metabolites in human whole blood using LC-ESI-MS/MS. *Ther Drug Monit* **34:**134-142.

Edgar RC (2013) UPARSE: highly accurate OTU sequences from microbial amplicon reads. *Nat Methods* **10:**996-998.

Floren LC, Bekersky I, Benet LZ, Mekki Q, Dressler D, Lee JW, Roberts JP, and Hebert MF (1997) Tacrolimus oral bioavailability doubles with coadministration of ketoconazole. *Clin Pharmacol Ther* **62:**41-49.

Goulet M, Rupprecht K, Sinclar P, Wyvratt M, and Parsons W (1994) The medicinal chemistry of FK-506. *Perspectives in Drug Discovery and Design* **2:**145.

Haiser HJ, Gootenberg DB, Chatman K, Sirasani G, Balskus EP, and Turnbaugh PJ (2013) Predicting and manipulating cardiac drug inactivation by the human gut bacterium Eggerthella lenta. *Science* **341:**295-298.

Ianiri G, Applen Clancey S, Lee SC, and Heitman J (2017) FKBP12-Dependent Inhibition of Calcineurin Mediates Immunosuppressive Antifungal Drug Action in Malassezia. *MBio* **8**.

Koppel N, Maini Rekdal V, and Balskus EP (2017) Chemical transformation of xenobiotics by the human gut microbiota. *Science* **356**.

Lee JR, Magruder M, Zhang L, Westblade LF, Satlin MJ, Robertson A, Edusei E, Crawford C, Ling L, Taur Y, Schluter J, Lubetzky M, Dadhania D, Pamer E, and Suthanthiran M (2018) Gut microbiota dysbiosis and diarrhea in kidney transplant recipients. *Am J Transplant*.

Lee JR, Muthukumar T, Dadhania D, Taur Y, Jenq RR, Toussaint NC, Ling L, Pamer E, and Suthanthiran M (2015) Gut microbiota and tacrolimus dosing in kidney transplantation. *PLoS One* **10:**e0122399.

Lopez-Siles M, Martinez-Medina M, Abella C, Busquets D, Sabat-Mir M, Duncan SH, Aldeguer X, Flint HJ, and Garcia-Gil LJ (2015) Mucosa-associated Faecalibacterium prausnitzii phylotype richness is reduced in patients with inflammatory bowel disease. *Appl Environ Microbiol* **81:**7582-7592.

McCabe M, Sane RS, Keith-Luzzi M, Xu J, King I, Whitcher-Johnstone A, Johnstone N, Tweedie DJ, and Li Y (2015) Defining the Role of Gut Bacteria in the Metabolism of Deleobuvir: In Vitro and In Vivo Studies. *Drug metabolism and disposition: the biological fate of chemicals* **43:**1612-1618.

Messele T, Roos MT, Hamann D, Koot M, Fontanet AL, Miedema F, Schellekens PT, and Rinke de Wit TF (2000) Nonradioactive techniques for measurement of in vitro T-cell proliferation: alternatives to the [(3)H]thymidine incorporation assay. *Clin Diagn Lab Immunol* **7:**687-692.

Miquel S, Leclerc M, Martin R, Chain F, Lenoir M, Raguideau S, Hudault S, Bridonneau C, Northen T, Bowen B, Bermudez-Humaran LG, Sokol H, Thomas M, and Langella P (2015) Identification of metabolic signatures linked to anti-inflammatory effects of Faecalibacterium prausnitzii. *MBio* **6**.

Moller A, Iwasaki K, Kawamura A, Teramura Y, Shiraga T, Hata T, Schafer A, and Undre NA (1999) The disposition of 14C-labeled tacrolimus after intravenous and oral administration in healthy human subjects. *Drug Metab Dispos* **27:**633-636.

Namiki Y, Kihara N, Koda S, Hane K, and Yasuda T (1993) Tautomeric phenomenon of a novel potent immunosuppressant (FK506) in solution. I. Isolation and structure determination of tautomeric compounds. *J Antibiot (Tokyo)* **46:**1149-1155.

Press RR, Ploeger BA, den Hartigh J, van der Straaten T, van Pelt J, Danhof M, de Fijter JW, and Guchelaar HJ (2009) Explaining variability in tacrolimus pharmacokinetics to optimize early exposure in adult kidney transplant recipients. *Ther Drug Monit* **31:**187-197.

Qin J, Li R, Raes J, Arumugam M, Burgdorf KS, Manichanh C, Nielsen T, Pons N, Levenez F, Yamada T, Mende DR, Li J, Xu J, Li S, Li D, Cao J, Wang B, Liang H, Zheng H, Xie Y, Tap J, Lepage P, Bertalan M, Batto JM, Hansen T, Le Paslier D, Linneberg A, Nielsen HB, Pelletier E, Renault P, Sicheritz-Ponten T, Turner K, Zhu H, Yu C, Li S, Jian M, Zhou Y, Li Y, Zhang X, Li S, Qin N, Yang H, Wang J, Brunak S, Dore J, Guarner F, Kristiansen K, Pedersen O, Parkhill J, Weissenbach J, Meta HITC, Bork P, Ehrlich SD, and Wang J (2010) A human gut microbial gene catalogue established by metagenomic sequencing. *Nature* **464:**59-65.

Rossi O, van Berkel LA, Chain F, Tanweer Khan M, Taverne N, Sokol H, Duncan SH, Flint HJ, Harmsen HJ, Langella P, Samsom JN, and Wells JM (2016) Faecalibacterium prausnitzii A2-165 has a high capacity to induce IL-10 in human and murine dendritic cells and modulates T cell responses. *Sci Rep* **6:**18507.

Schroeder BO and Backhed F (2016) Signals from the gut microbiota to distant organs in physiology and disease. *Nat Med* **22:**1079-1089.

Sender R, Fuchs S, and Milo R (2016) Revised Estimates for the Number of Human and Bacteria Cells in the Body. *PLOS Biology* **14:**e1002533.

Shuker N, van Gelder T, and Hesselink DA (2015) Intra-patient variability in tacrolimus exposure: causes, consequences for clinical management. *Transplant Rev (Orlando)* **29:**78-84.

Sokol H, Pigneur B, Watterlot L, Lakhdari O, Bermudez-Humaran LG, Gratadoux JJ, Blugeon S, Bridonneau C, Furet JP, Corthier G, Grangette C, Vasquez N, Pochart P, Trugnan G, Thomas G, Blottiere HM, Dore J, Marteau P, Seksik P, and Langella P (2008) Faecalibacterium prausnitzii is an anti-inflammatory commensal bacterium identified by gut microbiota analysis of Crohn disease patients. *Proc Natl Acad Sci U S A* **105:**16731-16736.

Sousa T, Paterson R, Moore V, Carlsson A, Abrahamsson B, and Basit AW (2008) The gastrointestinal microbiota as a site for the biotransformation of drugs. *Int J Pharm* **363:**1-25.

Staatz CE and Tett SE (2004) Clinical pharmacokinetics and pharmacodynamics of tacrolimus in solid organ transplantation. *Clin Pharmacokinet* **43:**623-653.

Steinbach WJ, Reedy JL, Cramer RA, Jr., Perfect JR, and Heitman J (2007) Harnessing calcineurin as a novel anti-infective agent against invasive fungal infections. *Nat Rev Microbiol* **5:**418-430.

Tatusova T, Ciufo S, Fedorov B, O'Neill K, and Tolstoy I (2014) RefSeq microbial genomes database: new representation and annotation strategy. *Nucleic Acids Res* **42:**D553-559.

Tuteja S, Alloway RR, Johnson JA, and Gaber AO (2001) The effect of gut metabolism on tacrolimus bioavailability in renal transplant recipients. *Transplantation* **71:**1303-1307.

Venkataramanan R, Swaminathan A, Prasad T, Jain A, Zuckerman S, Warty V, McMichael J, Lever J, Burckart G, and Starzl T (1995) Clinical pharmacokinetics of tacrolimus. *Clin Pharmacokinet* **29:**404-430.

Wallace BD, Wang H, Lane KT, Scott JE, Orans J, Koo JS, Venkatesh M, Jobin C, Yeh LA, Mani S, and Redinbo MR (2010) Alleviating cancer drug toxicity by inhibiting a bacterial enzyme. *Science* **330:**831-835.

Yu LX, Crison JR, and Amidon GL (1996) Compartmental transit and dispersion model analysis of small intestinal transit flow in humans. *International Journal of Pharmaceutics* **140:**111-118.

Footnotes

This work was supported by National Institute of Health [K23 AI 124464] (J.R.L.) and Chicago Biomedical Consortium [Catalyst Award C-066] (H.J.).

J.R.L. receives research support from BioFire Diagnostics, LLC. The other authors of this manuscript have no conflicts of interest to disclose as described by the Drug Metabolism and Disposition.

Yukuang Guo and Camila Manoel Crnkovic contributed equally.

Figure legends

Fig 1. *F. prausnitzii* metabolizes tacrolimus. A, *F. prausnitzii* (OD_{600} 2.6) cultured in YCFA media was incubated with tacrolimus (100 μg/ml) anaerobically at 37°C for 48 h. The mixture was analyzed by using HPLC/UV. B, Time profiles of tacrolimus disappearance and M1 appearance upon anaerobic incubation of tacrolimus (100 μg/ml) with *F. prausnitzii*.

Fig 2. Chemical structures of tacrolimus and *F. prausnitzii*-derived metabolite M1. M1 structure was identified using mass spectrometry and nuclear magnetic resonance spectroscopy.

Fig 3. M1 is less potent than tacrolimus as an immunosuppressant and antifungal agent. A, Immunosuppressant activities of tacrolimus and M1 were examined in PBMCs by measuring cell proliferation after treatment with a T-lymphocyte mitogen in the presence of tacrolimus or M1. B, Antifungal activities of tacrolimus and M1 were examined using *Malassezia sympodialis*. The yeast was inoculated on mDixon agar plate. After 1 h incubation, an aliquot of tacrolimus or M1 at different concentrations was placed on the plate as shown on the left panel and incubated at 37°C for 2 days.

Fig 4. Multiple commensal gut bacteria convert tacrolimus to M1. A, Representative chromatograms of bacteria incubated with tacrolimus. M1 non-producer (*B. longum*) or producers (*C. aldenense, C. citroniae, and Erysipelotrichaceae sp*.) cultured overnight in YCFA media was incubated with tacrolimus (100 μg/ml) anaerobically at 37°C for 48 h. The mixture was analyzed by using HPLC/UV at 210 nm. B, Mouse or human hepatic microsomes (HM; 3 mg microsomal protein/ml) were incubated with tacrolimus (100 μg/ml) at 37°C for 2 h aerobically. The mixture was analyzed by using HPLC/UV.

Fig 5. Human gut microbiota convert tacrolimus to M1. Tacrolimus (100 μg/ml) was incubated anaerobically with human stool samples from two different subjects (100 mg wet weight/ml) for 48 h at 37°C. A separate set of sample was boiled for 10 min before incubation with tacrolimus. The incubation mixtures were analyzed by HPLC/UV.

Fig 6. M1 formation in small intestinal bacteria may be extensive. A, Tacrolimus (10 μg/ml) was incubated anaerobically with varying amounts of *F. prausnitzii* in PBS at 37°C for 2 h. B, Tacrolimus (10

μg/ml) was incubated with *F. prausnitzii* (6.3×10^7 cells/ml) for varying time. C, Tacrolimus at varying concentrations was incubated with *F. prausnitzii* (6.3×10^7 cells/ml) for 1 h. M1 concentrations in the reaction mixtures were analyzed by LC-MS/MS.

DMD Fast Forward. Published on December 31, 2018 as DOI: 10.1124/dmd.118.084772
This article has not been copyedited and formatted. The final version may differ from this version.

Table 1. Screening gut bacteria for tacrolimus conversion to M1 in YCFA culture

Order	Bacterium	OD_{600}	M1 production detected
Bifidobacteriales	*Bifidobacterium longum*	1.8	No
Bacteroidales	*Bacteroides cellulosilyticus*	0.6	Yes[a]
	Bacteroides finegoldii	3.4	Yes[a]
	Bacteroides ovatus	4.2	Yes[a]
	Parabacteroides merdae	2.7	Yes[a]
	Parabacteroides johnsonii	3.6	Yes[a]
	Parabacteroides goldsteinii	3.3	Yes[a]
Clostridiales	*Ruminococcaceae sp.*	0.5	Yes
	Clostridium innocuum	3.4	Yes
	Anaerostipes sp.	2.7	Yes
	Dorea formicigenerans	2.4	Yes
	Clostridium clostridioforme	3.0	Yes
	Clostridium hathewayi	2.6	Yes
	Blautia sp.	4.7	Yes
	Clostridium aldenense	1.4	Yes
	Clostridium symbiosum	2.5	Yes
	Clostridium citroniae	1.7	Yes
	Coprococcus sp.	2.4	Yes
	Clostridium bolteae	3.6	Yes
	Clostridium cadaveris	1.4	Yes
	Ruminococcus gnavus	3.4	Yes
Erysipelotrichales	*Erysipelotrichaceae sp.*	3.8	Yes

[a], M1 production observed only when using a sensitive LC/MS/MS for detection.

DMD Fast Forward. Published on December 31, 2018 as DOI: 10.1124/dmd.118.084772
This article has not been copyedited and formatted. The final version may differ from this version.

Table 2. M1 levels in kidney transplant patients' stool samples.

Patient ID	Age (years)	Gender	Post-transplant Day	Tacrolimus oral dose[a] (mg/day)	Fecal abundance of *F. prausnitzii*	Fecal abundance of *Clostridiales*	Baseline tacrolimus level in stool samples (ng/mg stool)	Baseline M1 level in stool samples (ng/mg stool)	M1 production upon tacrolimus incubation (ng/mg stool)
1	45	Female	31	9	46%	86%	0.88	0.38	5.1
2	56	Male	18	3	39%	89%	BQL[c]	BQL[d]	3.5
3	61	Male	20	5	32%	71%	0.63	BQL[d]	4.5
4	59	Female	12	6	27%	76%	0.71	0.12	2.9
5	50	Male	32	10	26%	79%	0.37	0.41	6.4
6	52	Female	28	6	ND[b]	15%	0.29	BQL[d]	3.5
7	57	Male	15	3	ND[b]	44%	0.85	BQL[d]	4.1
8	71	Male	18	4	ND[b]	95%	BQL[c]	0.60	7.1
9	25	Male	27	4	ND[b]	74%	0.49	BQL[d]	12.6
10	52	Male	32	6	ND[b]	95%	0.14	BQL[d]	11.0

[a], at the time of stool collection
[b], not detected
[c], below the quantification limit (i.e., 0.1 ng/mg stool)
[d], below the quantification limit (i.e., 0.1 ng/mg stool)

DMD Fast Forward. Published on December 31, 2018 as DOI: 10.1124/dmd.118.084772
This article has not been copyedited and formatted. The final version may differ from this version.

Fig 1

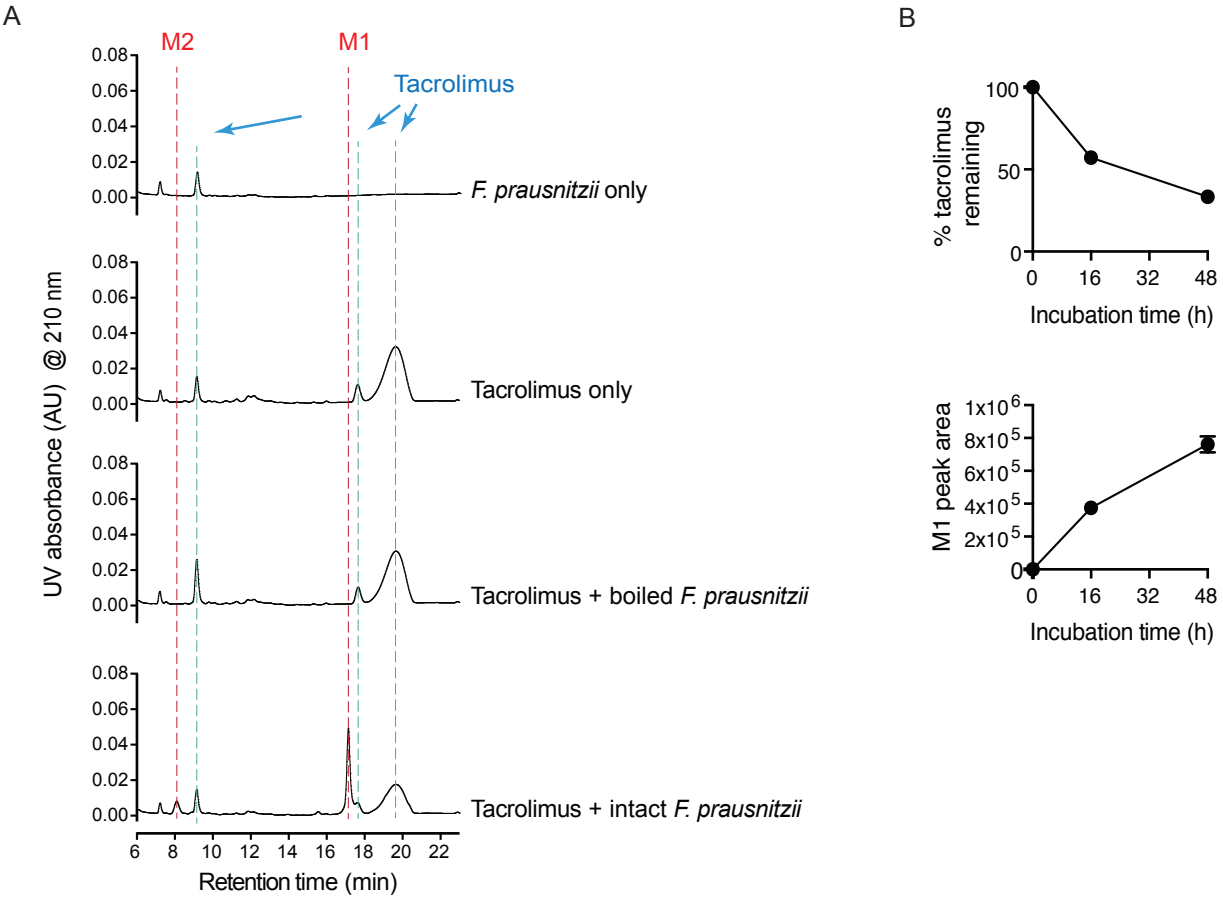

DMD Fast Forward. Published on December 31, 2018 as DOI: 10.1124/dmd.118.084772
This article has not been copyedited and formatted. The final version may differ from this version.

Fig 2

Tacrolimus

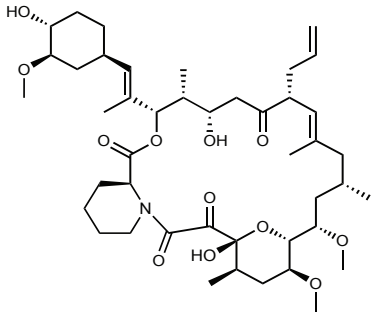

M1

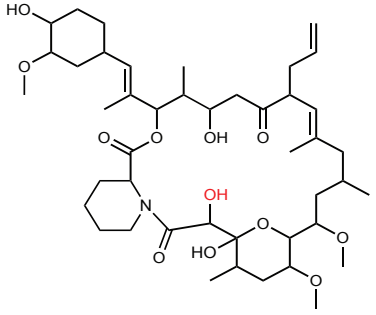

DMD Fast Forward. Published on December 31, 2018 as DOI: 10.1124/dmd.118.084772
This article has not been copyedited and formatted. The final version may differ from this version.

Fig 3

A

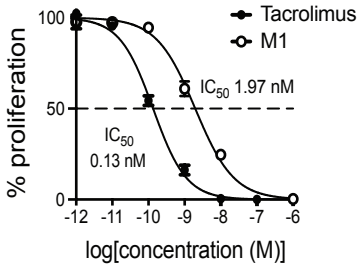

B

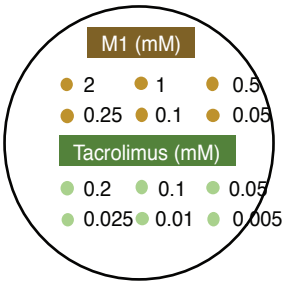

DMD Fast Forward. Published on December 31, 2018 as DOI: 10.1124/dmd.118.084772
This article has not been copyedited and formatted. The final version may differ from this version.

Fig 4

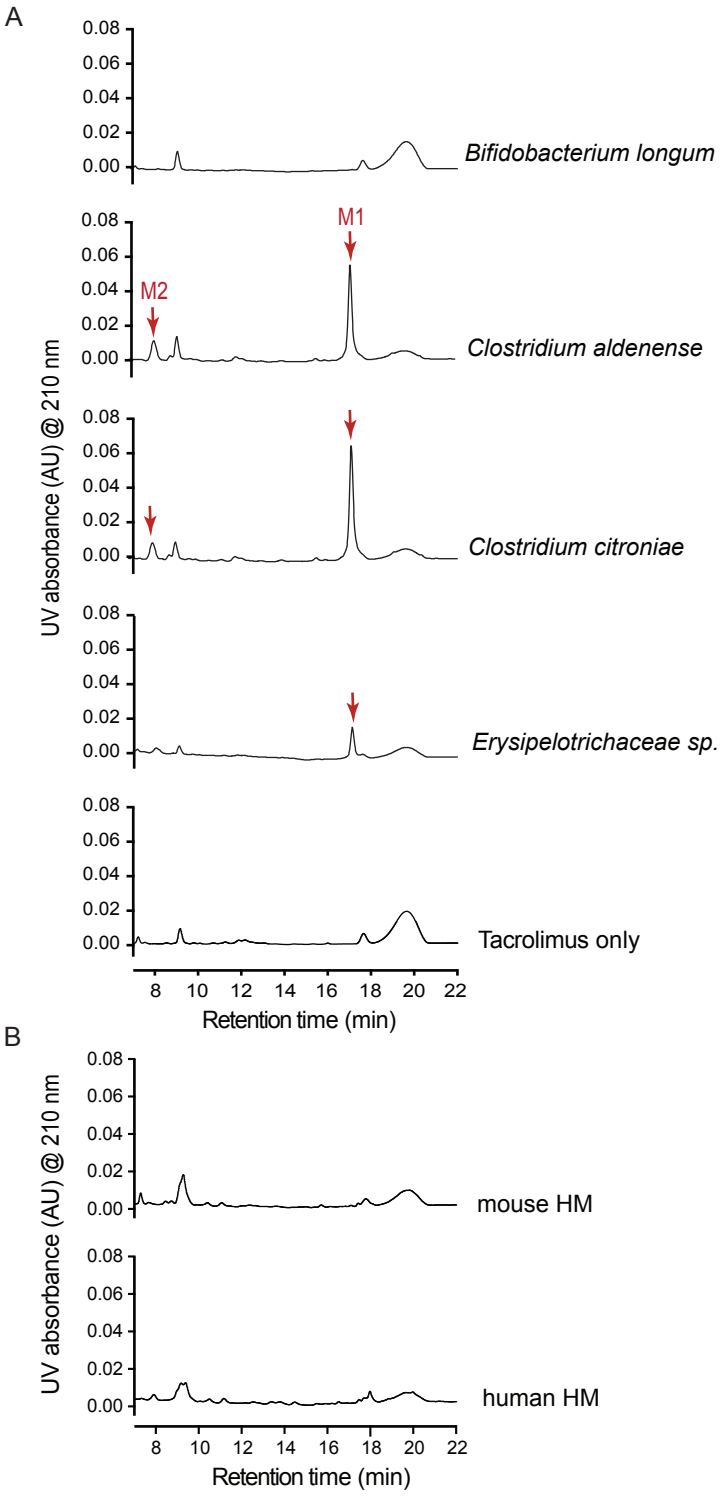

DMD Fast Forward. Published on December 31, 2018 as DOI: 10.1124/dmd.118.084772
This article has not been copyedited and formatted. The final version may differ from this version.

Fig 5

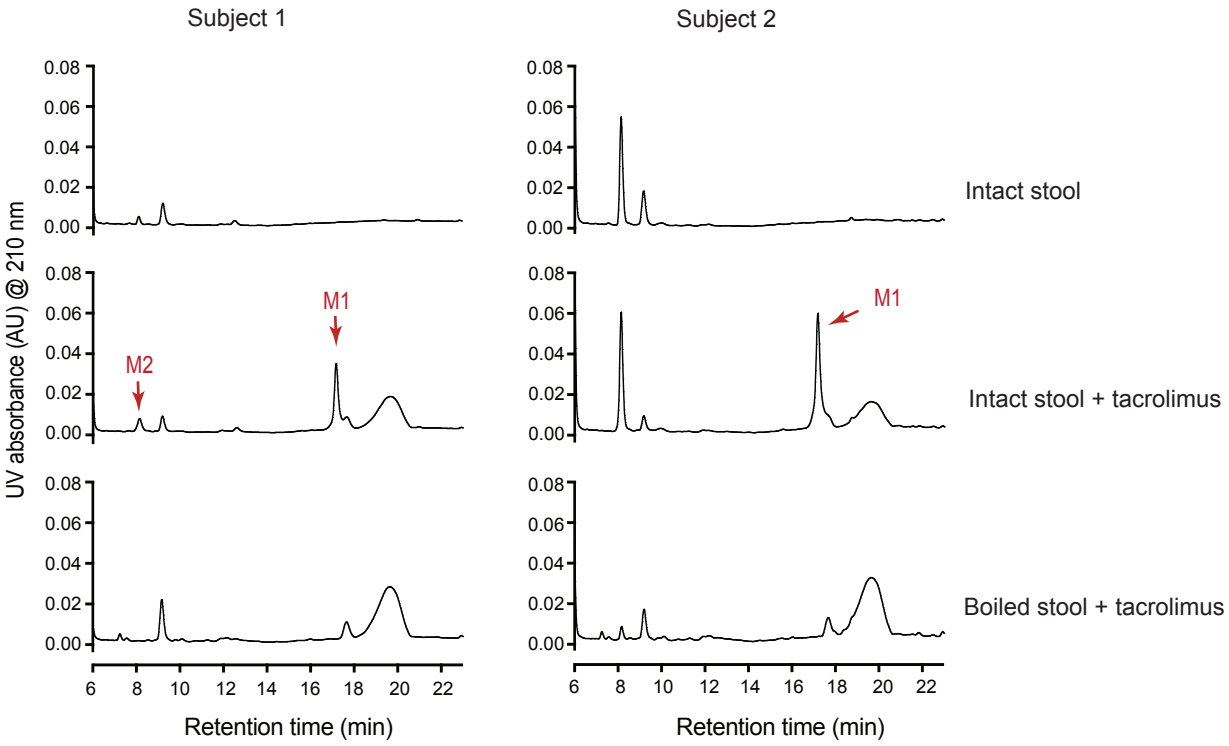

DMD Fast Forward. Published on December 31, 2018 as DOI: 10.1124/dmd.118.084772
This article has not been copyedited and formatted. The final version may differ from this version.

Fig 6

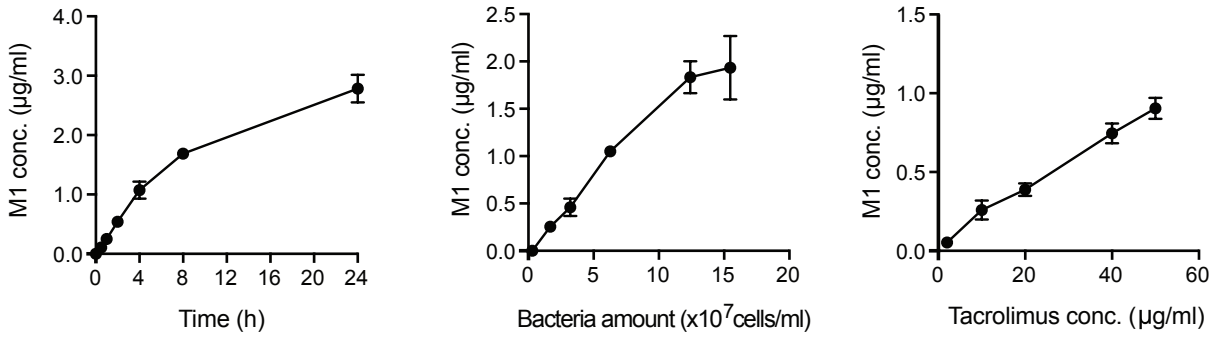

Supplemental information

Commensal gut bacteria convert the immunosuppressant tacrolimus to less potent metabolite

Yukuang Guo[1,5,a], Camila Crnkovic[1,a], Kyoung-Jae Won[2], John Richard Lee[3], Jimmy Orjala[1,5], Hyunwoo Lee[1,5], and Hyunyoung Jeong[2,4,5]

[1,] Department of Medicinal Chemistry and Pharmacognosy, University of Illinois at Chicago
[2,] Department of Pharmacy Practice, University of Illinois at Chicago
[3,] Division of Nephrology and Hypertension, Department of Medicine, Weill Cornell Medicine
[4,] Department of Biopharmaceutical Sciences, University of Illinois at Chicago
[5,] Center for Biomolecular Sciences

[a,] both authors contributed equally

Journal Title: Drug Metabolism and Disposition

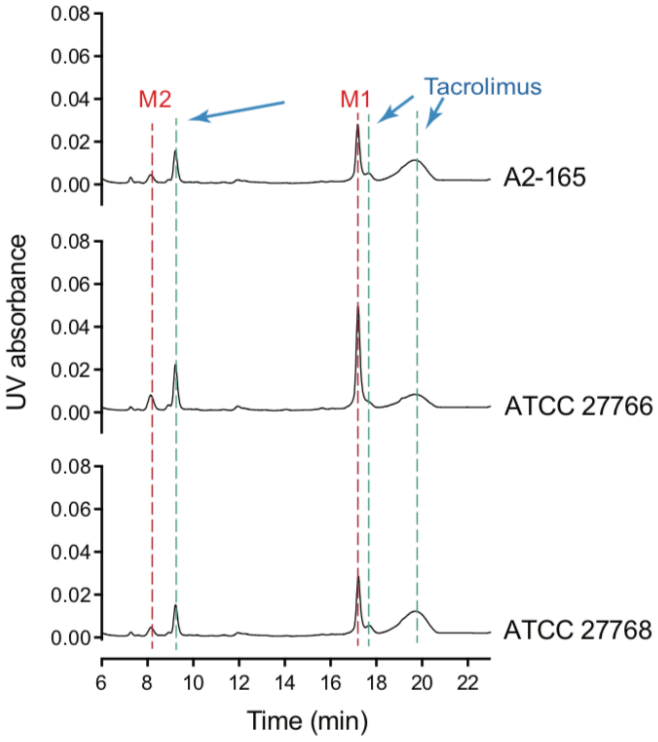

Supplemental Fig 1. Different strains of *F. prausnitzii* (i.e., A2-165, ATCC 27766 and ATCC 27768) were cultured overnight in YCFA media, followed by anaerobic incubation with tacrolimus (100 μg/ml) at 37°C for 48 h. The mixture was analyzed by using HPLC-UV at 210 nm.

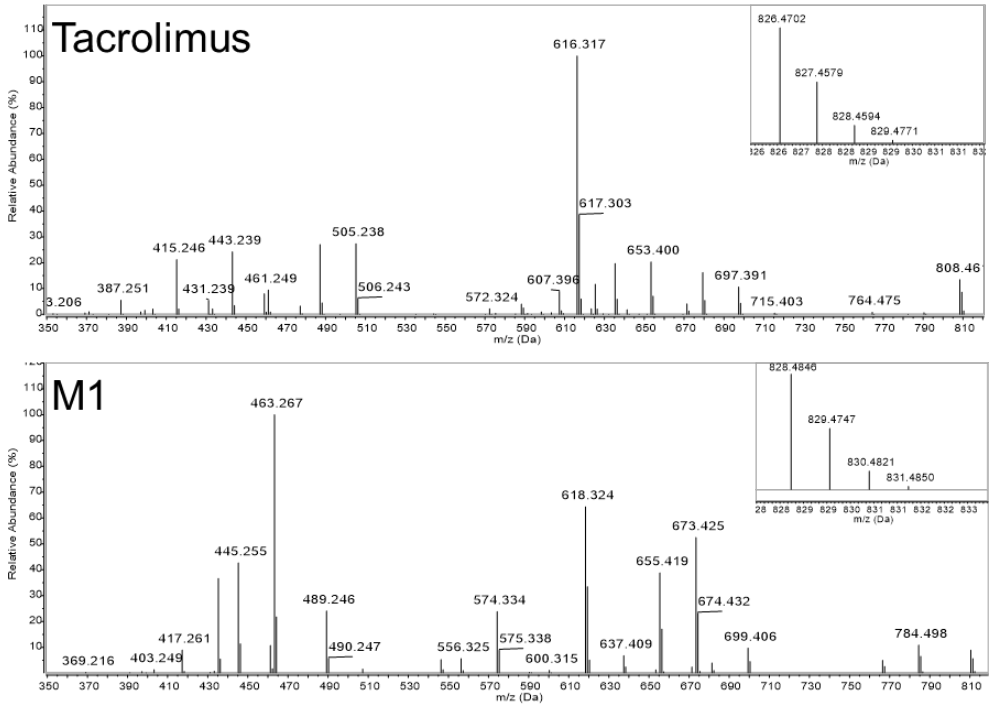

Supplemental Fig 2. MS^2 spectra of tacrolimus and M1 (IT-TOF)

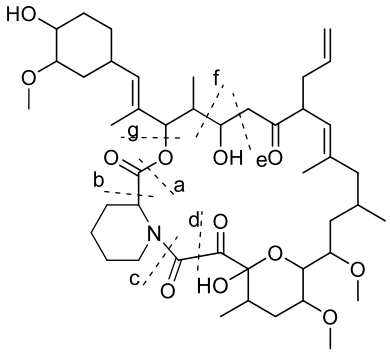

Tacrolimus fragmentation

	Tacrolimus			**M1**		
[Ion + Na]$^+$	Calc. *m/z*	IT-TOF	QTOF	Calc. *m/z*	IT-TOF	QTOF
M	826.4717	826.4702	826.4692	828.4874	828.4846	828.4889
M-H$_2$O	808.4612	808.460	808.4589	810.4768	810.478	810.4645
M-2H$_2$O	790.4506	790.455		792.4663		
a-c	715.4033	715.403	715.4153	717.4190		717.4116
a-c-H$_2$O	697.3928	697.391	697.3919	699.4084	699.406	699.4103
a-c-2H$_2$O	679.3822	679.380	679.3885	681.3979	681.397	
g-d	671.4135	671.410		673.4292	673.425	
g-d-H$_2$O	653.4029	653.400	653.4029	655.4186	655.419	655.4230
g-d-2H$_2$O	635.3924	635.388	635.3983	637.4080	637.409	
f-g	616.3098	616.317	616.3092	618.3254	618.324	618.3274
f-a	598.2992	598.299	598.2940	600.3149	600.315	
f-b	572.3199	572.324	572.3102	574.3356	574.334	572.3380
f-c	487.2308	489.229	487.2259	489.2464	489.246	489.2615
f-d	461.2515	461.249	461.2524	463.2672	463.267	463.2670
f-d-H$_2$O	443.2410	443.239	443.2420	445.2566	445.255	445.2614
e-g	588.3149	588.315	588.3163	590.3305	590.351	590.3219
e-d	431.2410	431.239	431.2437	433.2566	433.254	433.2625
	433.2566	433.257	433.2556	435.2723	435.272	435.2743
	415.2460	415.246	415.2469	417.2617	417.261	417.2579
	371.2198		371.2194	371.2198		371.2145
	353.2093		353.2137	353.2093		353.2051
	261.1467		261.1431	261.1467		261.1449
[Ion + H]$^+$						
Piperidine	84.0813		84.0803	84.0813		84.0794
Pipecolic acid	130.0868		130.0873	130.0868		130.0862

Supplemental Fig 3. MS^2 fragments of tacrolimus and M1 obtained in IT-TOF and QTOF systems

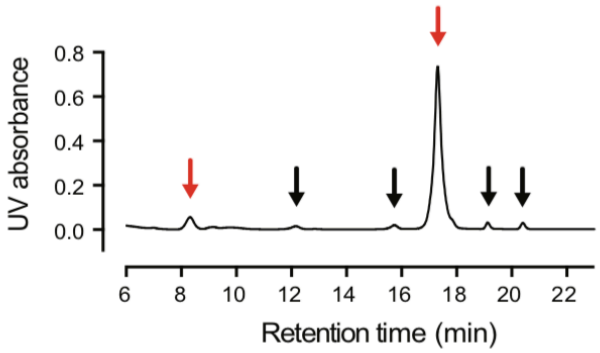

Supplemental Fig 4. Tacrolimus (50 mg) was incubated with *F. prausnitzii* A2-165 (OD ~2; 500 ml) for 96 h, followed by ethyl acetate extraction of the mixture. The fraction for M1 was isolated by using HPLC, combined, dried, and reconstituted in methanol. An aliquot (1 µl) was analyzed by HPLC-UV. Red arrows denote the retention times for M2 and M1. Black arrows denote retention times for potential M1 isomers.

a)

b)

c)

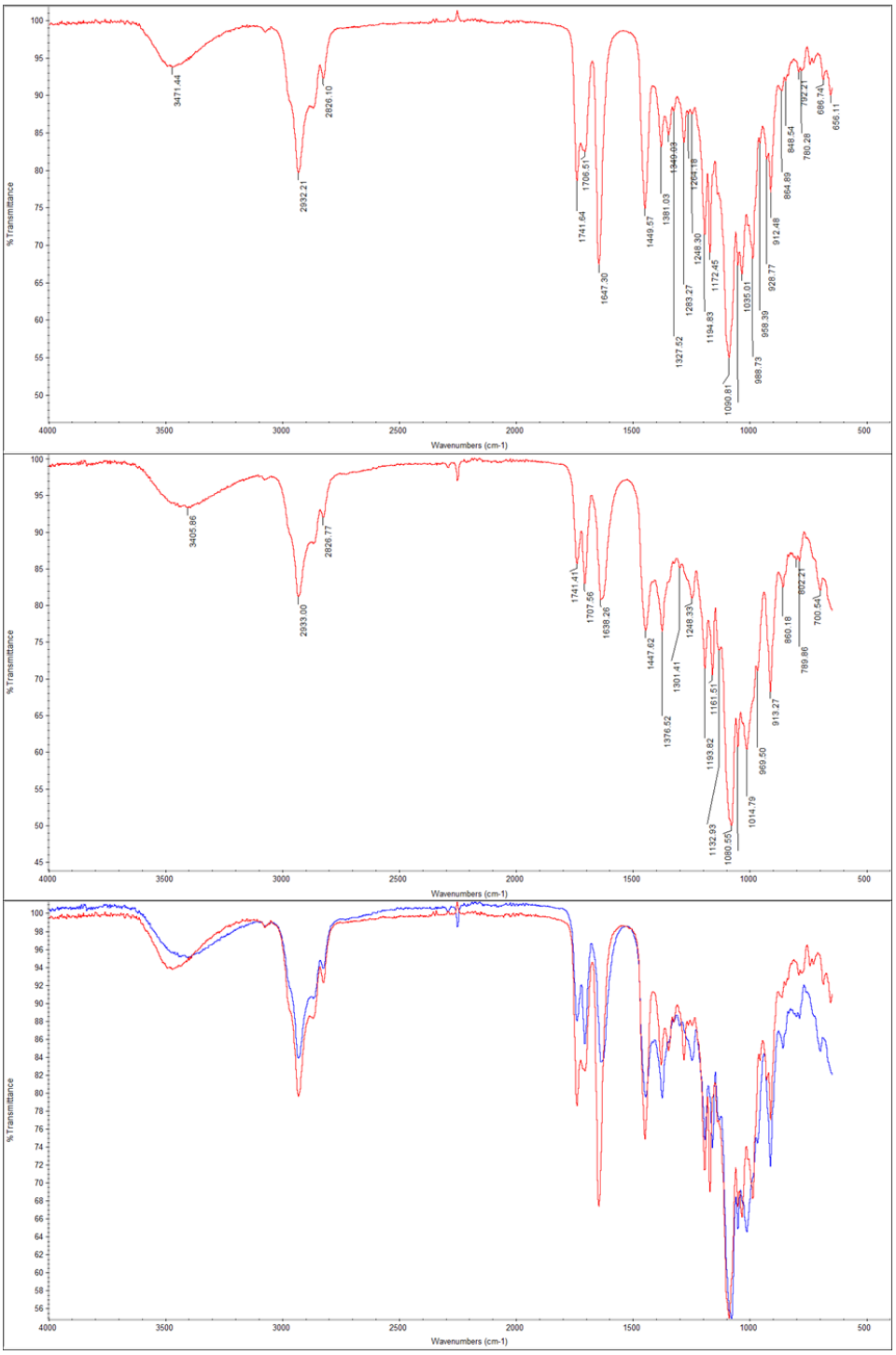

Supplemental Fig 5. IR spectra of a) tacrolimus, b) M1, c) overlay of tacrolimus (red) and M1 (blue) spectra

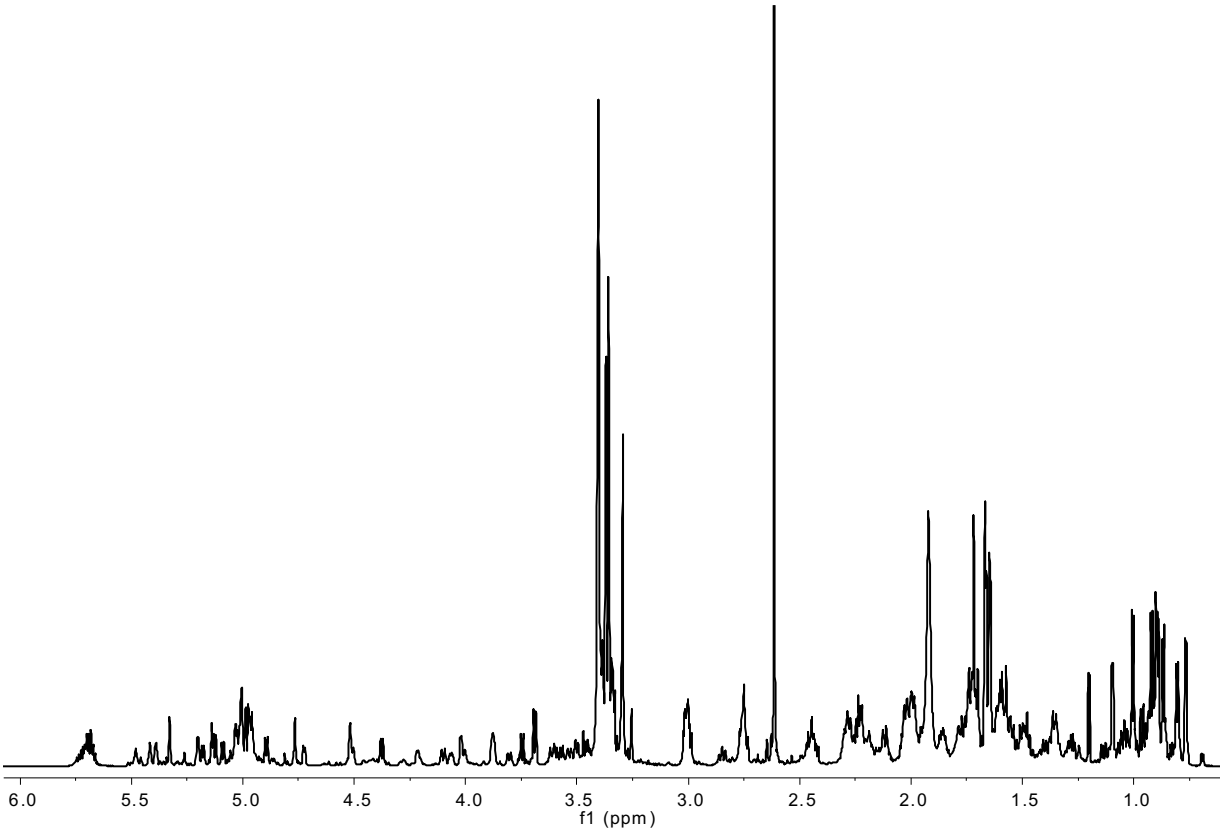

Supplemental Fig 6. ^{1}H NMR spectrum (900 MHz, $CDCl_3$) of M1

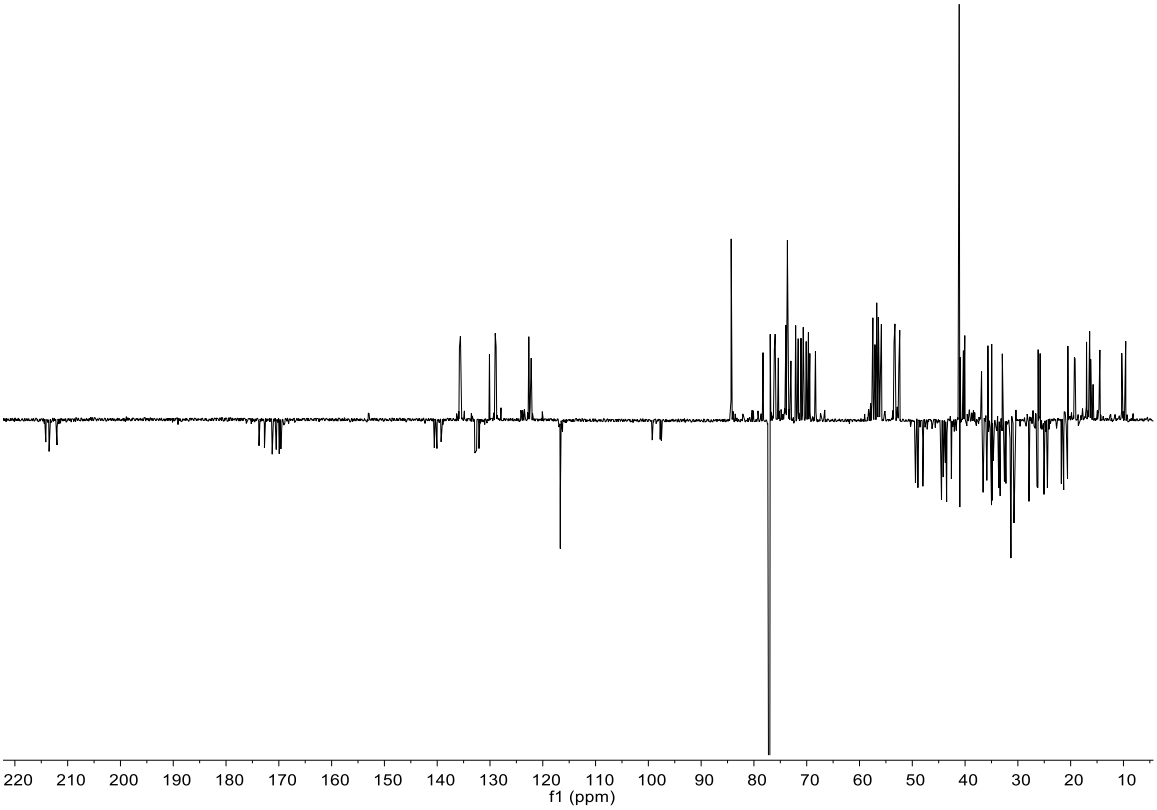

Supplemental Fig 7. DEPTQ spectrum (226 MHz, $CDCl_3$) of M1

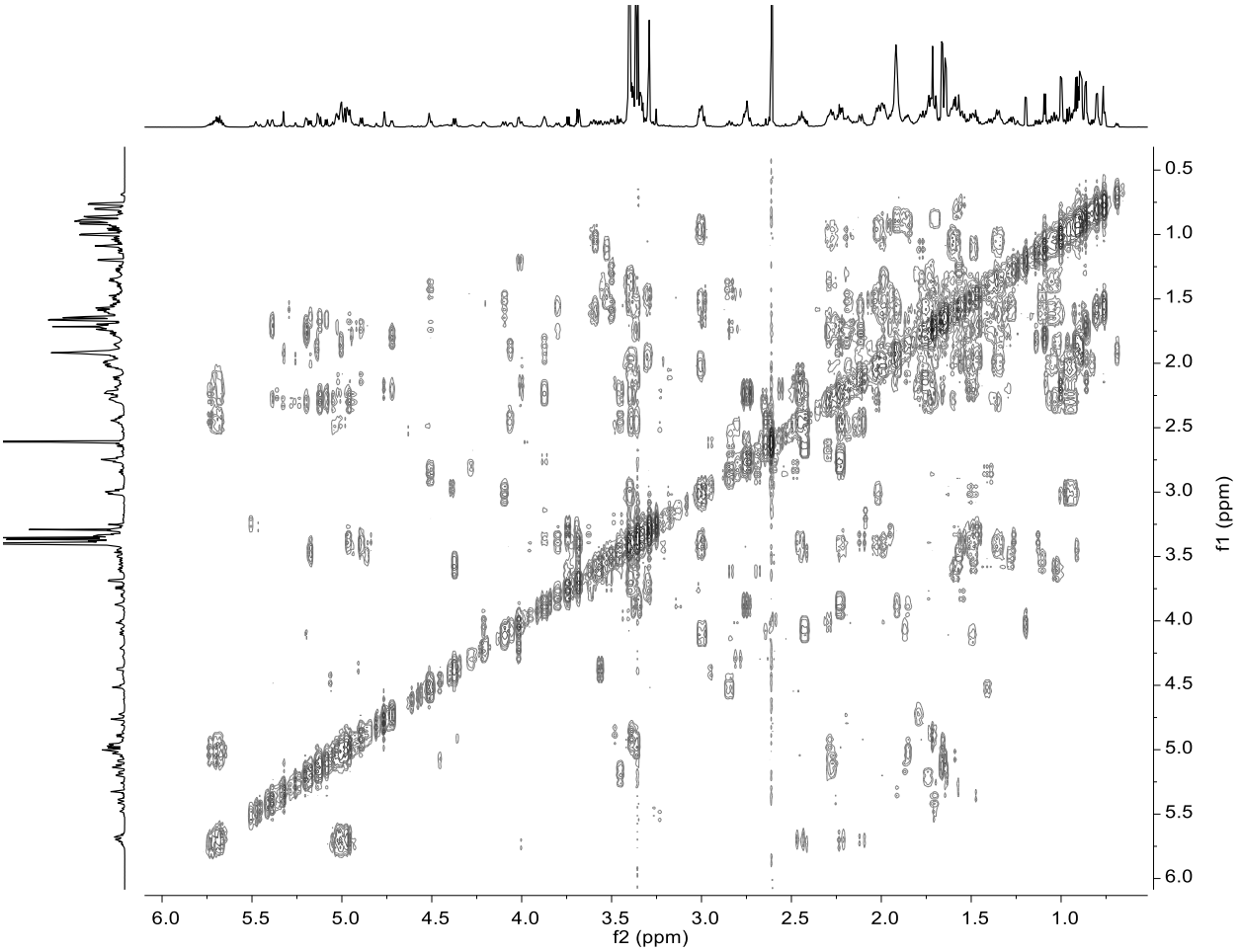

Supplemental Fig 8. COSY spectrum (900 MHz, $CDCl_3$) of M1

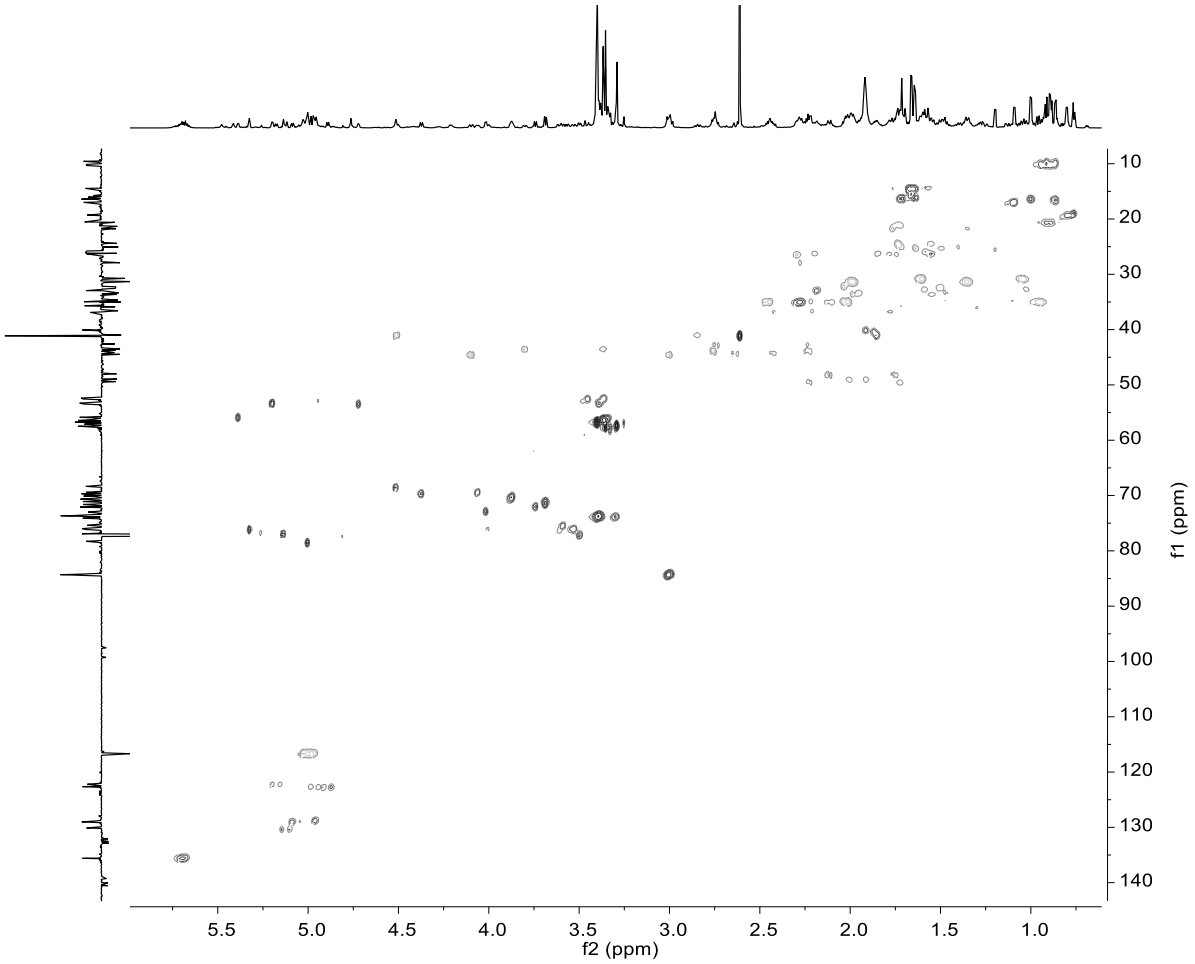

Supplemental Fig 9. HSQC spectrum (900 MHz, $CDCl_3$) of M1

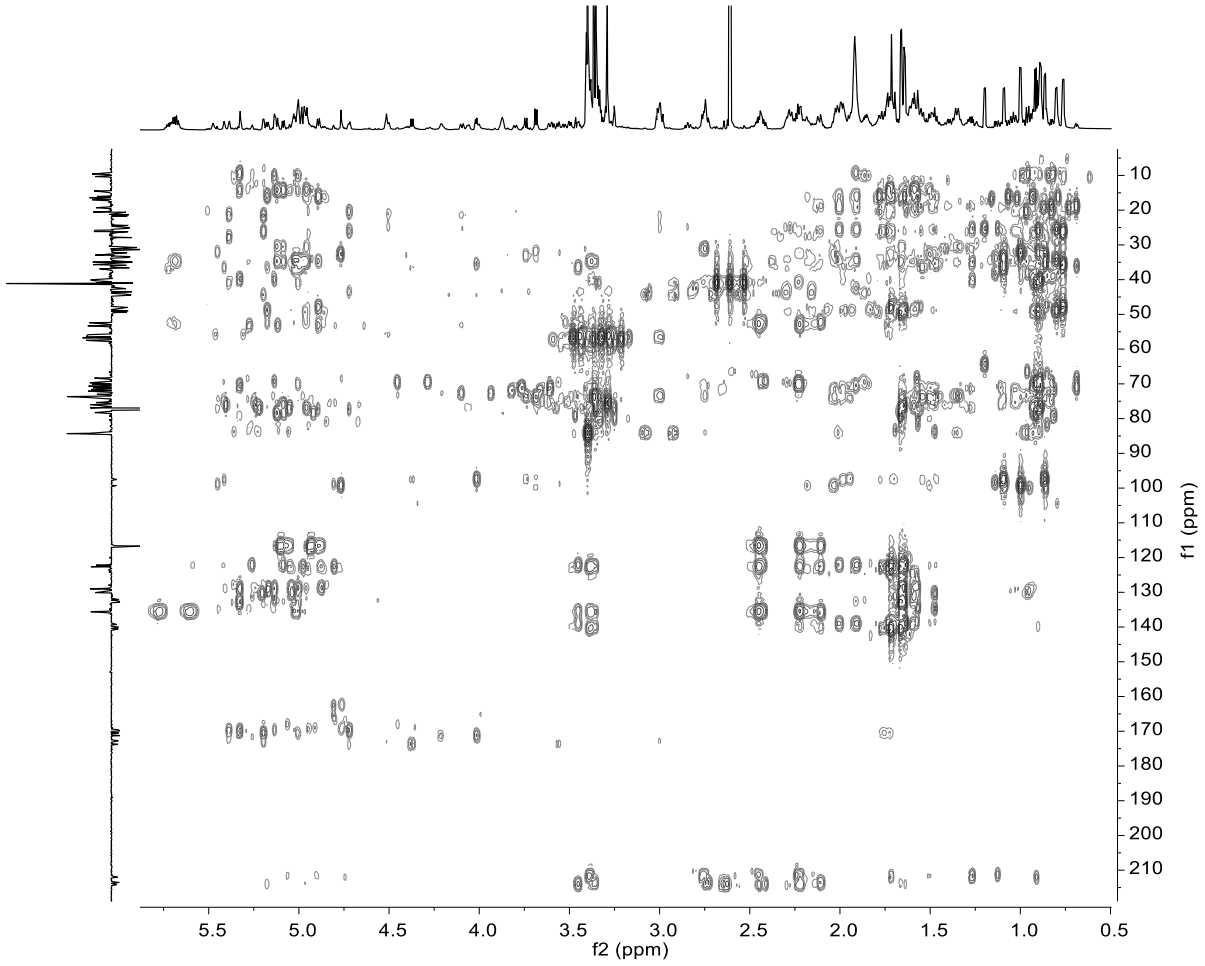

Supplemental Fig 10. HMBC spectrum (900 MHz, $CDCl_3$) of M1

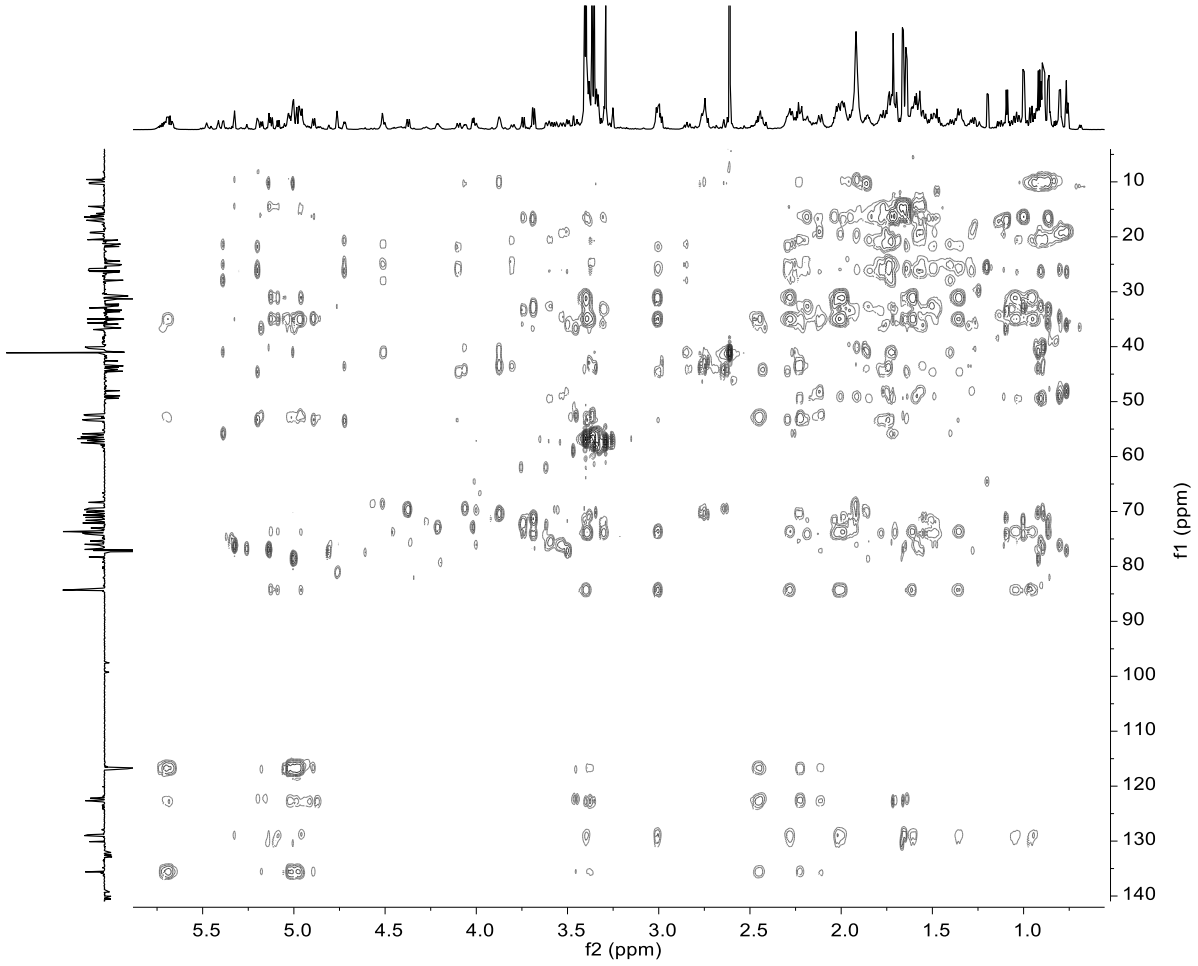

Supplemental Fig 11. ^{1}H-^{13}C HSQC-TOCSY spectrum (900 MHz, $CDCl_3$, 90 ms mixing time) of M1

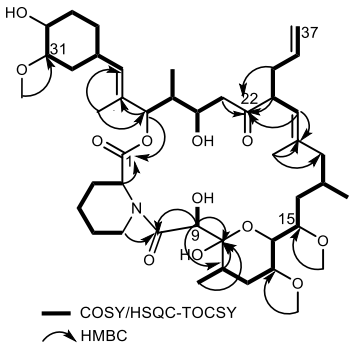

Supplemental Fig 12. Key 2D NMR correlations of M1 (Isomer I)

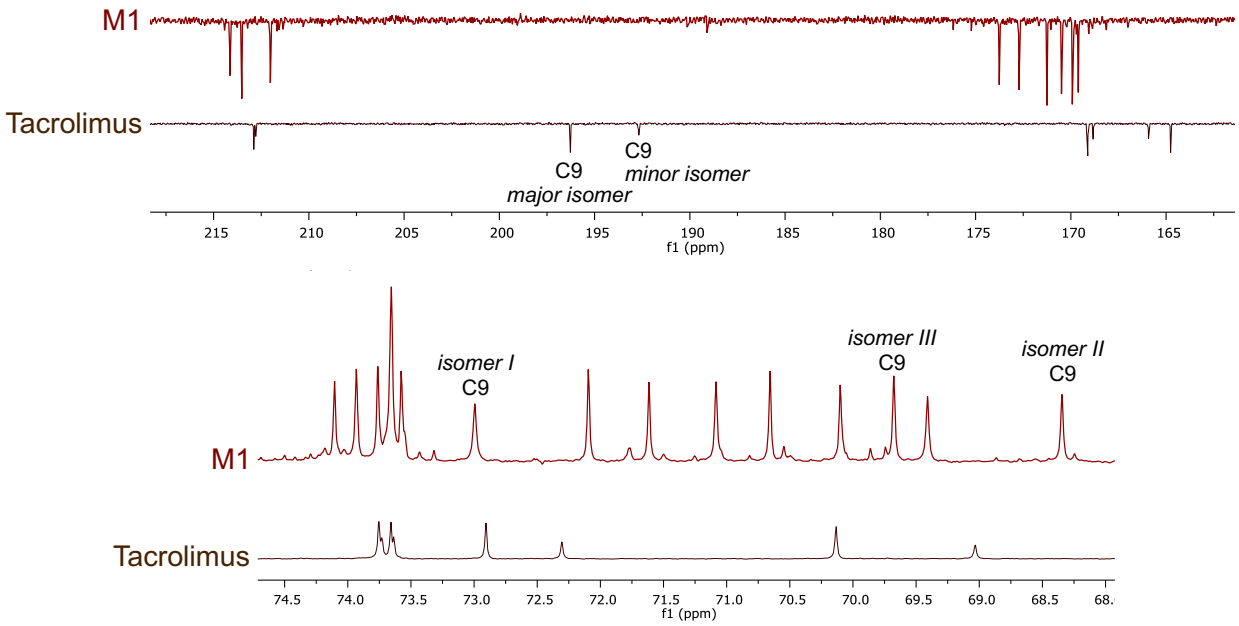

Supplemental Fig 13. Expansions of the DEPTQ spectra (226 MHz, CDCl3) of M1 (three major isomers assigned) and tacrolimus (two isomers)

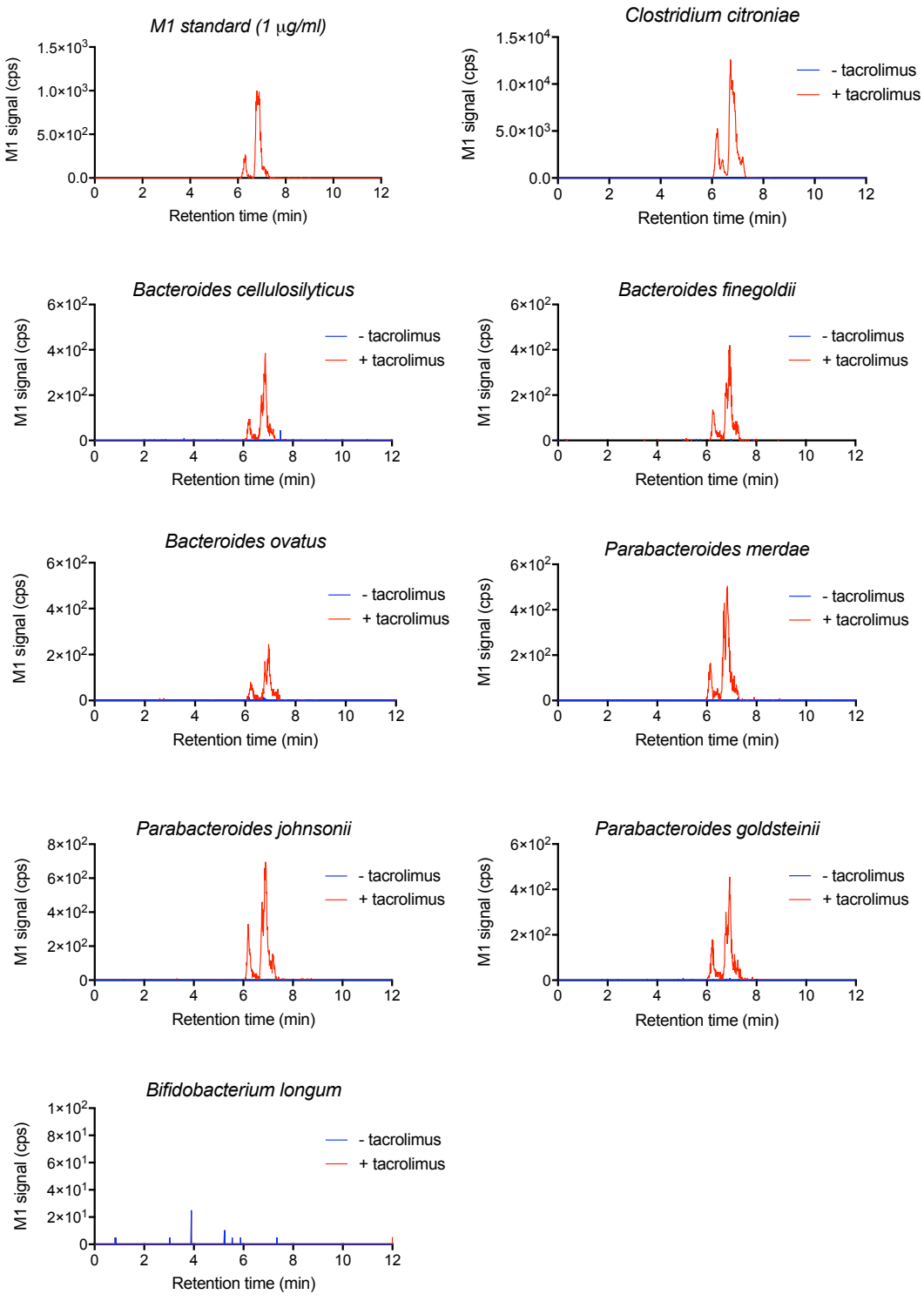

Supplemental Fig 14. Bacteria cultured overnight in YCFA media were incubated with tacrolimus (100 μg/ml) or vehicle control anaerobically at 37°C for 48 h. The mixtures were analyzed by HPLC/MS/MS (Applied Biosystems 3200Qtrap).

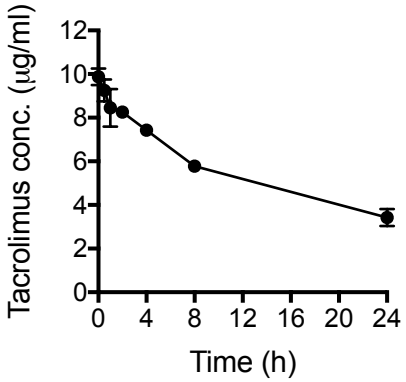

Supplemental Fig 15. Tacrolimus (10 μg/ml) was incubated with *F. prausnitzii* (6.28×10^{7} CFU/ml) anaerobically at 37°C up to 24 h. Tacrolimus concentration was analyzed by LC-MS/MS. Data shown are mean ± standard deviation of triplicate experiments.

Supplemental Table 1**.** List of commensal gut bacteria obtained from Biodefense and Emerging Infections (BEI) Research Resources Repository

	BEI catalog #	Bacterium	Strain	Order	OD_{600} Value
1	HM-845	*Bifidobacterium longum*	44B	*Bifidobacteriales*	1.78
2	HM-222	*Bacteroides ovatus*	3_8_47FAA	*Bacteroidales*	4.22
3	HM-726	*Bacteroides cellulosilyticus*	CL02T12C19	*Bacteroidales*	0.56
4	HM-727	*Bacteroides finegoldii*	CL09T03C10	*Bacteroidales*	3.44
5	HM-729	*Parabacteroides merdae*	CL09T00C40	*Bacteroidales*	2.71
6	HM-731	*Parabacteroides johnsonii*	CL02T12C29	*Bacteroidales*	3.56
7	HM-1050	*Parabacteroides goldsteinii*	CC87F	*Bacteroidales*	3.30
8	HM-79	*Ruminococcaceae sp.*	D16	*Clostridiales*	0.51
9	HM-173	*Clostridium innocuum*	Strain 6_1_30	*Clostridiales*	3.41
10	HM-220	*Anaerostipes sp.*	F0357	*Clostridiales*	2.69
11	HM-300	*Dorea formicigenerans*	4_6_53AFAA	*Clostridiales*	2.37
12	HM-306	*Clostridium clostridioforme*	2_1_49FAA	*Clostridiales*	2.98
13	HM-308	*Clostridium hathewayi*	WAL-18680	*Clostridiales*	2.63
14	HM-1032	*Blautia sp.*	KLE 1732	*Clostridiales*	4.65
15	HM-307	*Clostridium aldenense*	WAL-18727	*Clostridiales*	1.40
16	HM-309	*Clostridium symbiosum*	WAL-14163	*Clostridiales*	2.50
17	HM-315	*Clostridium citroniae*	WAL-17108	*Clostridiales*	1.65
18	HM-794	*Coprococcus sp.*	HPP0048	*Clostridiales*	2.36
19	HM-1038	*Clostridium bolteae*	CC43	*Clostridiales*	3.59
20	HM-1039	*Clostridium cadaveris*	CC40	*Clostridiales*	1.40
21	HM-1056	*Ruminococcus gnavus*	CC55_001C	*Clostridiales*	3.40
22	HM-180	*Erysipelotrichaceae sp.*	6_1_45	*Erysipelotrichales*	3.83

Supplemental Table 2. Demographic information of kidney transplant patients whose stool samples were analyzed

Patient ID	African American (AA) race	Type of transplant [a]
1	AA	LRT
2	Other	LRT
3	Other	LRT
4	AA	LRT
5	AA	LRT
6	AA	DDRT
7	AA	DDRT
8	Other	DDRT
9	Other	LRT
10	Other	DDRT

[a] LRT= living renal transplantation; DDRT = deceased donor renal transplantation

Supplemental Table 3. NMR spectroscopic data of M1 (Isomer I), $CDCl_3$[a]

Position	δ_C, mult[b]	δ_H (mult, *J* in Hz)[b,c]	COSY	HSQC-TOCSY (H→C)	HMBC (H→C)
1	169.6, C	-			
2	55.9, CH	5.39 (d, 4.5)	3, 6	3, 4, 5, 6	1, 3, 4
3	27.9, CH_2	2.26, 1.70	2, 4	2, 4, 6	5
4	21.3, CH_2	1.80, 1.40	3, 5, 6	2, 3, 5, 6	
5	25.1, CH_2	1.73, 1.70	4, 6	2, 3, 6	
6	41.0, CH_2	4.51, 2.85	2, 4, 5	2, 3, 4, 5	2, 4, 5, 8
8	171.3, C	-			
9	73.0, CH	4.02 (d, 6.5)	4.23		8, 10, 11
10	97.5, C	-			
11	35.7, CH	1.70	5.40, 12, 11-Me	12, 13, 11-Me	10, 11-Me
11-Me	16.4, CH_3	0.86 (d, 6.6)	11	11, 12, 13, 14	10, 11, 12
12	33.4, CH_2	1.96, 1.47	11, 13	14, 11-Me	10, 11, 13
13	73.7, CH	3.30	12, 14	11, 12, 14	15
13-OMe	56.3-56.4, CH_3	3.35-3.37			13
14	72.1, CH	3.74 (d, 9.8)	13, 15	12, 13, 11-Me	10, 12, 13
15	76.0, CH	3.53	14, 16	16, 17, 18, 17-Me	
15-OMe	57.6, CH_3	3.35			15
16	34.7, CH_2	1.48, 1.10 (d, 3.6)	15, 17	15, 17, 18, 17-Me	17, 18, 17-Me
17	25.8, CH	1.58	16, 18, 17-Me	17-Me	16, 18
17-Me	19.3, CH_3	0.80 (d, 6.5)	17	15, 16, 17, 18	16, 17, 18
18	48.9, CH_2	2.00, 1.91	17	17, 17-Me	17, 19, 17-Me
19	139.3, C	-			
19-Me	16.0, CH_3	1.64 (s)	20	20, 21	18, 19, 20, 22
20	122.2, CH	5.18 (d, 8.7)	21, 19-Me	21, 35, 36, 37, 19-Me	21, 22, 35
21	52.6, CH	3.45, (d, 8.2)	20, 35	20, 35, 36, 37	19, 20, 22, 35, 36
22	214.1, C	-			
23	44.1, CH_2	2.63 (d, 17.3), 2.43	24	24, 25-Me	22
24	69.4, CH	4.06 (dd, 10.3, 4.6)	3.41, 23, 25	23, 25, 25-Me	22, 26, 25-Me
25	40.3, CH	1.87	24, 26, 25-Me	24, 26, 25-Me	23, 24, 27, 25-Me
25-Me	10.3, CH_3	0.90	25	24, 25, 26	24, 25, 26
26	76.9, CH	5.13	25	25, 25-Me	1, 24, 25, 27, 28, 25-Me
27	132.1, C	-			
27-Me	14.5-14.6, CH_3	1.66	28	26, 28	26, 27, 28
28	128.8, CH	4.96	29, 27-Me	29/30, 31, 32, 33/34, 27-Me	26, 27, 29/30, 33/34, 27-Me
29	35.0, CH	2.30	28, 30, 34	28, 30, 31, 32, 33/34, 27-Me	
30	34.9-35.0, CH_2	2.01-2.04, 0.95	29, 31	28, 29, 31, 32, 33/34	31, 32
31	84.3, CH	3.00	30, 32	28, 29/30, 32, 33/34	32, 33, 31-OMe
31-OMe	56.7-56.8, CH_3	3.40			31
32	73.8, CH	3.39	31, 33	28, 29/30, 31, 33/34	31
33	31.3, CH_2	1.99, 1.35	32, 34	28, 29/30, 31, 32, 34	29/30, 31
34	30.7-30.8, CH_2	1.61, 1.04	29, 33	28, 29/30, 31, 32, 33	29
35	36.6, CH_2	2.44, 2.23	21, 36	20, 21, 36, 37	20, 21, 22, 36, 37
36	135.6, CH	5.71	35, 37	20, 21, 35, 37	21, 35
37	116.9, CH_2	4.98, 5.01	36	20, 21, 35, 36	35

[a] Frequencies of 900 MHz for ^1H and 226 MHz for ^{13}C

[b] A range of values (-) is indicated for chemical shifts that are interchangeable among isomers

[c] Peak multiplicity and coupling constants (*J*) are only reported for non-overlapping peaks on the ^1H spectrum

Supplemental Table 4. NMR Spectroscopic Data of M1 (Isomer II), $CDCl_3$[a]

Position	δ_C, mult[b]	δ_H (mult, *J* in Hz)[b,c]	COSY	HSQC-TOCSY (H→C)	HMBC (H→C)
1	170.5, C	-			
2	53.3, CH	5.20 (d, 5.5)	3, 6	3, 4, 5, 6	1, 3, 4, 6
3	26.4, CH_2	2.29, 1.74	2, 4	2, 4, 6	6
4	21.8, CH_2	1.77, 1.35	3	2, 6	
5	25.2, CH_2	1.64, 1.49	6	2, 3, 4, 6	
6	44.5, CH_2	4.10 (br d, 13.6), 2.99	2, 5	2, 3, 4, 5	2, 5, 8
8	172.7, C	-			
9	68.4, CH	4.51	3.21		8, 10
10	99.3, C	-			
11	33.0, CH	2.19	4.77, 12, 11-Me	13, 14, 11-Me	10, 11-Me
11-Me	16.4, CH_3	1.00 (d, 6.8)	11	11/12, 13, 14	10, 11/12
12	32.3, CH_2	2.04, 1.50	11, 13	13, 14, 11-Me	10
13	74.1, CH	3.39	12, 14	14, 11-Me	
13-OMe	56.3-56.4, CH_3	3.35-3.37			13
14	71.6, CH	3.68 (d, 9.6)	13, 15	13, 11-Me	10
15	77.1, CH	3.50	14, 16	14, 16, 17, 18, 17-Me	
15-OMe	57.6, CH_3	3.35			15
16	35.9, CH_2	1.56, 1.28	15, 17	15, 17, 18, 17-Me	14, 15, 17-Me
17	26.3, CH	1.55	16, 18, 17-Me	15, 18, 17-Me	18
17-Me	19.2, CH_3	0.76 (d, 6.3)	17	15, 16, 17, 18	16, 17, 18
18	48.0, CH_2	2.11, 1.75	17	17, 17-Me	17, 19, 17-Me
19	140.5, C	-			
19-Me	16.1, CH_3	1.71 (s)	20	20, 21	18, 19, 20, 22
20	122.7, CH	4.89 (d, 9.6)	21, 19-Me	21, 35, 36, 37, 19-Me	21, 22, 35, 36, 37
21	53.3, CH	3.39	20, 35	20, 35, 36, 37	19, 22, 35, 36
22	212.0, C	-			
23	43.7, CH_2	2.76, 2.23	24	24, 25-Me	22
24	70.1, CH	3.87	3.36, 23, 25	23, 25, 25-Me	23, 26
25	41.0, CH	1.85	24, 26, 25-Me	24, 26, 25-Me	23, 24, 27, 25-Me
25-Me	10.1, CH_3	0.92	25	24, 25, 26	24, 25, 26
26	78.3, CH	5.00	25	25, 28, 25-Me	1, 24, 25, 27, 28, 25-Me, 27-Me
27	132.5, C	-			
27-Me	14.5-14.6, CH_3	1.67	28	26, 28	26, 27, 28
28	130.1, CH	5.12 (d, 9.1)	29, 27-Me	29/30, 31, 32, 33/34, 27-Me	26, 27, 29/30, 33/34, 27-Me
29	35.0, CH	2.30	28, 30, 34	28, 30, 31, 32, 33/34, 27-Me	
30	34.9-35.0, CH_2	2.01-2.04, 0.95	29, 31	28, 29, 31, 32, 33/34	31, 32
31	84.2, CH	3.00	30, 32	28, 29/30, 32, 33/34	32, 33, 31-OMe
31-OMe	56.7-56.8, CH_3	3.40			31
32	73.7, CH	3.39	31, 33	28, 29/30, 31, 33/34	31
33	31.3, CH_2	1.99, 1.35	32, 34	28, 29/30, 31, 32, 34	29/30, 31
34	30.7-30.8, CH_2	1.61, 1.04	29, 33	28, 29/30, 31, 32, 33	29
35	34.9, CH_2	2.46, 2.23	21, 36	20, 21, 36, 37	20, 21, 22, 36, 37
36	135.6, CH	5.69	35, 37	20, 21, 35, 37	21, 35
37	116.7, CH_2	4.98, 5.01	36	20, 21, 35, 36	35

[a] Frequencies of 900 MHz for ^1H and 226 MHz for ^{13}C
[b] A range of values (-) is indicated for chemical shifts that are interchangeable among isomers
[c] Peak multiplicity and coupling constants (*J*) are only reported for non-overlapping peaks on the ^1H spectrum

Supplemental Table 5. NMR Spectroscopic Data of M1 (Isomer III), $CDCl_3$ [a]

Position	δ_C, mult[b]	δ_H (mult, *J* in Hz)[b,c]	COSY	HSQC-TOCSY (H→C)	HMBC (H→C)
1	169.9, C	-			
2	53.5, CH	4.72 (d, 6.5)	3, 6	3, 4, 5, 6	1, 3, 4, 6, 8
3	26.2, CH_2	2.20, 1.79	2, 4	2, 4, 5	1
4	20.6, CH_2	1.72, 1.28	3	2, 6	
5	24.4, CH_2	1.74, 1.55	6	2, 3, 6	
6	43.5, CH_2	3.80 (br d, 13.3), 3.37	2, 5	2, 3, 4, 5	2, 4, 5
8	173.8, C	-			
9	69.7, CH	4.37 (d, 10.3)	3.58		8, 10, 11
10	97.8, C	-			
11	36.9, CH	1.78	12, 11-Me	13	10
11-Me	17.0, CH_3	1.09 (d, 6.7)	11	11, 12, 13	10, 11, 12
12	33.6, CH_2	1.99, 1.54	11, 13	14	10, 13
13	73.9, CH	3.39	12, 14	14, 11-Me	
13-OMe	56.3-56.4, CH_3	3.35-3.37			13
14	71.1, CH	3.68 (d, 9.6)	13	13, 11-Me	10
15	75.4, CH	3.59	16	16, 17, 18, 17-Me	17-Me
15-OMe	57.6, CH_3	3.35			15
16	35.9, CH_2	1.56, 1.28	15, 17	15, 17, 18, 17-Me	14, 15, 17-Me
17	26.2, CH	1.85	16, 17-Me	16, 18, 17-Me	
17-Me	20.5, CH_3	0.90	17	15, 16, 17, 18	16, 17, 18
18	49.4, CH_2	2.23, 1.72	17	17-Me	19
19	140.1, C	-			
19-Me	15.8, CH_3	1.66 (s)	20	20, 21	18, 19, 20, 22
20	122.6, CH	4.97	21	21, 35, 36, 37, 19-Me	21, 22, 36
21	52.4, CH	3.36	20, 35	20, 35, 36, 37	19, 20, 22, 35, 36
22	213.5, C	-			
23	42.6, CH_2	2.74, 2.22	24	24, 25-Me	22
24	70.7, CH	3.87	3.12, 23, 25	23, 25, 25-Me	23, 26
25	40.1, CH	1.91	24, 26, 25-Me	24, 26, 25-Me	23, 24, 27, 25-Me
25-Me	9.6, CH3	0.89	25	24, 25, 26	24, 25, 26
26	76.1, CH	5.32	25	25, 28, 25-Me	1, 24, 25, 27, 28, 25-Me, 27-Me
27	132.9, C	-			
27-Me	14.5-14.6, CH3	1.65	28	26, 28	26, 27, 28
28	129.0, CH	5.09 (d, 9.1)	29, 27-Me	29/30, 31, 32, 33/34, 27-Me	26, 27, 29/30, 33/34, 27-Me
29	35.0, CH	2.27	28, 30, 34	28, 30, 31, 32, 33/34, 27-Me	
30	34.9-35.0, CH_2	2.01-2.04, 0.95	29, 31	28, 29, 31, 32, 33/34	31, 32
31	84.3, CH	3.00	30, 32	28, 29/30, 32, 33/34	32, 33, 31-OMe
31-OMe	56.7-56.8, CH_3	3.40			31
32	73.6, CH	3.39	31, 33	28, 29/30, 31, 33/34	31
33	31.3, CH_2	1.99, 1.37	32, 34	28, 29/30, 31, 32, 34	29/30, 31
34	30.7-30.8, CH_2	1.61, 1.04	29, 33	28, 29/30, 31, 32, 33	29
35	34.9, CH_2	2.46, 2.11	21, 36	20, 21, 36, 37	20, 21, 22, 36, 37
36	135.8, CH	5.69	35, 37	20, 21, 35, 37	21, 35
37	116.7, CH_2	4.98, 5.01	36	20, 21, 35, 36	35

[a] Frequencies of 900 MHz for ^{1}H and 226 MHz for ^{13}C

[b] A range of values (-) is indicated for chemical shifts that are interchangeable among isomers

[c] Peak multiplicity and coupling constants (*J*) are only reported for non-overlapping peaks on the ^{1}H spectrum